AN EVALUATION OF OMEGA WIND-FINDING ACCURACY USING STATIONARY DROPWINDSONDES

by

James Louis Franklin

B.S., Massachusetts Institute of Technology
(1980)

SUBMITTED IN PARTIAL FULFILLMENT
OF THE REQUIREMENTS OF THE DEGREE OF

MASTER OF SCIENCE
IN EARTH, ATMOSPHERIC, AND PLANETARY SCIENCE

at the

MASSACHUSETTS INSTITUTE OF TECHNOLOGY

September 1984

Signature of auth.....
Department of Earth, Atmospheric and Planetary Science
July 1, 1984

Certified by.....
Richard E. Passarelli
Thesis Supervisor

Accepted by.....
Theodore R. Madden
Chairman, Departmental Committee on Graduate Students

CONTENTS

AN EVALUATION OF OMEGA WIND-FINDING ACCURACY USING STATIONARY DROPWINDSONDES

by

JAMES LOUIS FRANKLIN

Submitted to the Department of Earth, Atmospheric, and Planetary Science on July 1, 1984 in partial fulfillment of the requirements for the degree of Master of Science in Earth, Atmospheric, and Planetary Science

ABSTRACT

The accuracy of wind estimates that have been derived from Omega signals was investigated using stationary dropwindsondes. Omega phases were collected for 145 min during two experiments in which NOAA aircraft flew patterns near dropwindsondes on the ground. Thus, actual Omega wind errors could be computed as the estimated wind speed. With this data set, the effect of aircraft maneuvers on Omega wind accuracy was documented, and the accuracy of three commonly used Omega phase-smoothing algorithms was evaluated over a range of signal qualities and station-sonde geometries. Noise-free synthetic Omega signals were used to estimate the relative resolution of the three algorithms.

Winds computed in real-time are shown to be greatly dependent on the motion of the aircraft receiving the Omega signals. During aircraft maneuvers (turns), wind errors increased by over 50%.

Wind estimates obtained using cubic-spline phase smoothing are shown to be 20-50% more accurate than estimates obtained using the other methods. The synthetic data show that quadratic smoothing has an inherently higher resolution than the spline; however, this advantage is negated by the presence of noise typically found in Omega signals. Hence it is recommended that cubic-spline phase smoothing be used in dropwindsonde postprocessing. It is estimated that postprocessing of dropwindsonde data using the cubic-spline algorithm will reduce wind errors by 60% during aircraft turns and by 30% at other times.

Thesis supervisor: Dr. Richard Passarelli

Title: Assistant Professor of Meteorology

I. INTRODUCTION

Omega dropwindsondes (ODW's) are instruments that are released from aircraft to obtain vertical profiles of pressure, temperature, humidity, and wind from otherwise data-sparse regions. Over 5000 such soundings are included in the First Global Atmospheric Research Program (GARP) Global Experiment (FGGE) data set (Julian, 1982). ODW's have been used in recent years over the Mediterranean Sea in GARP's 1982 Alpine Experiment (ALPEX), by the Atlantic Oceanographic and Meteorological Laboratory (AOML) Hurricane Research Division (HRD) to investigate the environmental flow of Hurricane Debby (1982), and by meteorologists to study the El Nino phenomenon in the eastern Pacific. Recently, researchers have been using ODW's in hopes of computing diagnostic quantities that require fairly precise measurements (El Nino, for example). ODW's have been used, or will be used, in the near future as input for important operational forecasting decisions regarding hurricanes and coastal winter storms, and they will continue to be a valuable tool until satellites can provide similar information. It is important, therefore, to understand the capabilities and limitations of this instrument. The accuracy and reliability of the thermodynamic measurements have been described by Franklin (1983). This study investigates the accuracy of ODW wind estimates.

To measure winds, ODW's use a network of eight very low frequency (13.6 kHz) transmitters, each of which broadcasts a 1 s pulse of energy every 10 s. Distance from one of these Omega stations to a sonde can be determined by measuring the signal phase of that station's transmission. As the sonde falls on a parachute (at 25-30 mb/min) it moves with the wind, and Omega signals relayed from the sonde from three or more stations provide an estimate of the sonde's horizontal position. Successive position estimates are used to estimate the horizontal wind. There are many valid methods of arriving at a vertical wind

profile from a set of phase measurements, the fundamental difference between these methods being how noise (always present in Omega data) is handled. Because of noise, individual phase measurements are not reliable enough to difference values, for example, 1 min apart, to get a 1-min average wind. It is necessary to somehow smooth each time series of phase values in order to obtain accurate estimates of the time rate of change of phase (Acheson, 1974). The manner in which this smoothing is done is a crucial factor in determining the character and accuracy of the estimated winds. One goal of this research is to evaluate three commonly-used smoothing algorithms that offer different approaches to this problem.

If the measurement error of an ODW wind estimate is defined to be $\{var(U)+var(V)\}^{1/2}$, then the equations that govern the solution of the horizontal winds also provide a solution for this error, or uncertainty in the wind estimate (Passi, 1977). For reasons discussed below, a quantity proportional to this uncertainty is usually calculated; hence, the uncertainty estimates of a given smoothing algorithm are generally calibrated empirically. A second goal of this work is to evaluate the accuracy of these uncertainty estimates and to suggest possible improvements, if necessary.

How accurate are Omega wind estimates is a commonly asked question that has no simple answer. Propagation characteristics vary with such factors as location on the globe, time of day, and even time of year. Signals may be degraded by interference from nearby machinery, by lightning hundreds or thousands of miles away, or by solar flares millions of miles away (Acheson, 1974). The spatial distribution of Omega stations around the sonde has a profound influence on wind accuracy. In the case of an airborne launch platform, computed winds are also affected by maneuvers of the aircraft. In most cases, interference, station geometry, and aircraft accelerations exert the strongest influence on Omega wind accuracy. The effects of these factors,

which are estimated by the wind uncertanties, are examined in this study.

Data from ODW's are available in real time. A computer on the aircraft receives raw signals from the falling sonde and converts them into measurements of pressure, temperature, and wind. These measurements are then displayed on the aircraft where they can be interpreted and relayed to forecasters and entered into the data base for operational models. (The wind-finder that is used to produce these real-time winds is one of the algorithms to be evaluated in this paper.) Although such real-time data can be extremely valuable to forecasters (as in the hurricane environment missions flown by HRD), many soundings contain errors that can be identified and corrected only with computing and graphics capabilities unavailable in the air. Thus, "postprocessing" of ODW data is generally advised (Franklin, 1983). The size of the on-board computer limits the sophistication of the airborne wind-finder, so the recording of phase data for postprocessing also allows the estimation of winds using a more complicated and possibly more accurate wind-finding algorithm on the ground. Knowledge of whether one algorithm is superior to the others would improve the accuracy of future postprocessed ODW data sets. By evaluating the accuracy of several competing wind-finders and their associated error estimates, the author expects that future ODW data sets will be more accurate and more readily interpreted than those in the past.

II. MATHEMATICAL BACKGROUND

At this point a discussion of the theory of Omega wind-finding is in order so that the reader may better understand the analysis that follows. Much of the derivation below can be found in Passi (1974) and Acheson (1974).

A. Equations

Consider k Omega stations S_j, j=1,k at longitudes a_j and latitudes b_j. If a dropwindsonde is at (longitude,latitude)=(x,y), the central earth angle f_j between station j and the sonde is given by

$$(1) \quad f_j=\cos^{-1}\{\cos(a_j-x)\cos(y)\cos(b_j)+\sin(y)\sin(b_j)\}$$

and the distance between the station j and the sonde is Rf_j, where R is the radius of the earth. If a transmitted wave W propagating from station j has a radial frequency w, wavelength L, and has zero phase at the transmitter at time t_1, then at time t the wave received at the sonde can be expressed as

$$(2) \quad T=\exp i\{(2\pi/L)s + w(t-t_1)\}$$

where s is the propagation path length equal to Rf_j. The signal phase at the sonde, $\phi_{sj}(t)$, is given by the ratio of the imaginary to the real part of (2):

$$(3) \quad \phi_{sj}(t)=2\pi Rf_j/L + w(t-t_1).$$

Omega signals are received by the sonde and retransmitted without modification to the launching aircraft. The signal phase at the aircraft, $\phi_j(t)$, will therefore be given by $\phi_{sj}(t)+c$,

where c is the change in phase that occurs between the sonde and the plane. ϕ_j is not the quantity that is measured on board, however, but rather a relative phase p_j, which is the signal phase ϕ_j minus a local oscillator phase. If we define p_{ij} as $p_i - p_j$, the phase difference between stations i and j, it can be shown easily that this difference of relative phases is equal to the difference of Omega signal phases $\phi_i - \phi_j$. It then follows quickly that

(4) $p_{ij} = \{2\pi R/L\} f_{ij}$, where $f_{ij} = f_i - f_j$, $i \neq j = 1,k$.

Such a set of equations is referred to as a hyperbolic set, for reasons that shall be clear momentarily. Rearranging (4) gives

(5) $(Rf_i - Rf_j) = (L/2\pi) p_{ij}$, $i \neq j = 1,k$.

We measure the right hand side of (5). Now the set of points that satisfy $(Rf_i - Rf_j)$ = a constant describe a hyperboloid. Another relative phase measurement p_{im}, $m \neq j$ defines a second hyperboloid, whose intersection with the first is a (nearly) vertical line. In this manner Omega signals from three stations define the (x,y) position of the sonde.

Only k-1 equations of (4) are independent. With no loss, therefore, we may set j=k:

(6) $p_{ik}(t) = (2\pi R/L) f_{ik}$, $i = 1,k-1$.

Differentiation with respect to t gives

$$\dot{p}_{ik} = \partial p_{ik}/\partial t = \frac{2\pi R}{L}\left\{\frac{\partial f_{ik}}{\partial x}\frac{\partial x}{\partial t} + \frac{\partial f_{ik}}{\partial y}\frac{\partial y}{\partial t}\right\}$$

and since $U = R\cos(y)\,\partial x/\partial t$ and $V = R\,\partial y/\partial t$, substitution gives

(7) $$\dot{p}_{ik} = \{2\pi/L\cos(y)\}\frac{\partial f_{ik}}{\partial x}U + \{2\pi/L\}\frac{\partial f_{ik}}{\partial y}V,\ i = 1,k-1$$

or in vector notation,

$$(8) \qquad \dot{\mathbf{p}} = \mathbf{F}\begin{bmatrix} U \\ V \end{bmatrix}.$$

It is the method of estimating $\dot{\mathbf{p}}$ that distinguishes the three wind-finding algorithms to be examined in this study. The estimating algorithm must serve two functions: noise removal in the phase data, and evaluation of the phase rates for different stations at a common time, since the eight stations transmit sequentially rather than simultaneously. Before entering into a discussion of these "phase smoothers," however, we shall proceed a bit further with the more general equations.

$\dot{\mathbf{p}}$ is generally represented as $\hat{\dot{\mathbf{p}}} + \mathbf{s}$, where $\hat{\dot{\mathbf{p}}}$ is the phase rate estimator and $\mathbf{s}$ is the matrix of phase-rate difference errors. Equation 8 then becomes

$$(9) \qquad \hat{\dot{\mathbf{p}}} + \mathbf{s} = \mathbf{F}\begin{bmatrix} U \\ V \end{bmatrix}.$$

For k Omega stations, (9) represents k-1 independent equations in two unknowns. Thus, for k>3 the system is overdetermined and the traditional solution (Julian, 1982) is

$$(10) \qquad \mathbf{U} = (\mathbf{F}^T\mathbf{E}^{-1}\mathbf{F})^{-1}\mathbf{F}^T\mathbf{E}^{-1}\hat{\dot{\mathbf{p}}},$$

where $\mathbf{E}$ is the covariance matrix of $\mathbf{s}$, and $\mathbf{U}=[U,V]^T$. $(\mathbf{F}^T\mathbf{E}^{-1}\mathbf{F})^{-1}$ represents the covariance matrix of $\mathbf{U}$ (Passi, 1977), so the wind uncertainty $WU=\{\text{Var } U + \text{Var } V\}^{1/2}$ equals the square root of the trace of this matrix.

How shall we estimate the elements of $\mathbf{E}$? Since $\mathbf{s}$ is made up of phase-rates, the elements e_{ij} should come from estimates of observed phase-rate errors. Standard procedure, however, is to estimate $\hat{\mathbf{p}}$ first (by fitting the raw phases to a quadratic, for example) and then to differentiate to obtain phase rates; hence, it is much more convenient to get phase errors (as

residuals from a quadratic least-squares fit, for example) than phase-rate errors. Passi argues that the covariance matrix **E** based on phase-rate errors would be proportional to one based on phase errors alone. This proportionality constant would fall out of (10) and not influence **U**, although it would affect the wind uncertainty WU. The covariance matrix **E** that Passi suggests is standard in many wind-finders. Its elements e_{ij} are given by

$$\begin{aligned} e_{ij} &= s_i^2 + s_k^2 \quad i=j \\ e_{ij} &= s_k^2 \quad i\neq j \end{aligned} \tag{11}$$

where the phase variance s^2 is given by

$$s^2 = \sum_{i=1}^{n} [p(t_i)-\hat{p}(t_i)]^2/(n-1) \tag{12}$$

and n is the total number of phase observations. The scaling of the wind uncertainties is accomplished by tracking ODW's with precision radars (Julian, 1983, private communication and Passi, 1977).

Having seen the basic equations used in Omega wind-finding, we can now look at the differences between some of these algorithms. As stated earlier, in this study we are interested in seeing whether any of three common phase-smoothing routines provide significantly more accurate wind estimates than the others. The three smoothers to be examined are a quadratic least-squares fit, application of a low-pass filter, and a cubic-spline fit to the phase data.

B. Quadratic Least-Squares Smoothing

The simplest of the three methods is a second-order least-

squares polynomial approximation to the phase data. Because of its simplicity, this routine is used to compute real-time winds on board the aircraft. In addition, this routine was used in the postprocessing of about half of the data from the Hurricane Debby HRD dropsonde missions (low-pass filtering was used on the rest) and with data sets processed by HRD for other scientists.

To evaluate winds at time T, 3 min of phase data (19 phase measurements) surrounding T are fit to a quadratic by the method of least-squares. A fit is done for each of the Omega stations to be used in the computation (up to a maximum of four in real time). Once the fitting polynomials are determined, one can analytically differentiate to obtain phase rates at time T. (The derivatives are evaluated at times slightly different from T to correct for the fact that Omega stations broadcast in sequence.) Phase variances are evaluated using residuals from the polynomial fit in (12) with n=19. This procedure is then repeated for time T+1Ø with the next 1Ø-s phase measurement at the center of a new 3-min window.

What are the limitations of this quadratic model? As a practical matter, since each wind evaluation occurs at the midpoint of a 3-min interval and the sonde falls at 25-35 mb/min, no winds can be computed until about 4Ø mb after launch and the procedure must stop about 5Ø mb before splash (or other loss of signal). No direct estimate of surface winds is therefore available. There are theoretical limitations as well. The quadratic approximation implies a constant component of acceleration toward each Omega station over a 3-min interval (Passi, 1977). For a sonde moving with the wind, this is a reasonable approximation; however, the measurement of signal phase does not take place at the sonde, but for dropwindsondes, on a moving aircraft. The relayed signal from the sonde thus reflects aircraft as well as sonde motion. When the aircraft turns, the restriction of constant acceleration implied by the quadratic is not satisfied. For this reason, required turns are executed just before the

launch of a sonde whenever possible. The least-squares fitting presents another problem as well. The overall slope of a low-order fit is rather sensitive to the location of the points near the ends of the fit. In unedited Omega where noise may be present, or in all Omega where aircraft turns have occurred, such irregularities in the signal could be expected to have a large impact on computed winds as the irregularities enter and exit the 3-min smoothing window. This "window-endpoint" effect is demonstrated in section IV.

C. Low-Pass Filtering

A wind-finder that uses low-pass filtering of Omega data is described by Julian (1982) and has been implemented at HRD. This procedure takes the entire phase sequence for each station and transforms it into frequency space using a fast Fourier transform. The transform is then multiplied by a low-pass filter function, a complex exponential $\exp(-i\omega r_j)$ to correct for the transmission time difference between stations, and by $i\omega$ to produce phase rates from phases. After experimentation with radar-tracked upsondes, Julian settled on a filter with a 4-min effective length.

This procedure seems to have certain advantages over quadratic smoothing. One would expect it to be less susceptible to unedited random noise than a quadratic, because much of the noise is explicitly filtered, and because there are no window-endpoint effects. This routine was used in HRD processing primarily with sondes with relatively poor Omega; much less erratic wind profiles resulted from this algorithm than from quadratic fits for these sondes. One drawback of this procedure, however, is that its 4-min filter length prevents the computation of winds over even larger intervals than the 3-min quadratic; these intervals are 60-70 mb thick with this method. It has

been, nonetheless, an excellent complement to the quadratic smoother for poorer quality signals.

D. Cubic-Spline Smoothing

The third algorithm examined in this study is described by Passi (1977) as a cubic spline smoother, although the method does not actually use a true spline. Cubic spline smoothing was used to process ALPEX Omega data at the National Center for Atmpspheric Research (NCAR), but not until recently was the method available at HRD. This routine first divides the entire phase sequence into segments of about 3-min. Cubic polynomials are then fit to each segment, with the restriction that adjacent cubics give the same phases, phase rates, and radial accelerations at the join points, or nodes. Specifically,

$$(13) \quad \hat{p} = \sum_{m=0}^{3} a_{jm} t^m = P_j(t), \quad T_{j-1} \leq t < T_j, \quad j=1,\ldots,N$$

describes the N cubics while the restrictions are given by

$$(14) \quad \partial^i P_{j-1}(T_{j-1})/\partial t^i = \partial^i P_j(T_{j-1})/\partial t^i, \quad i=0,1,2, \quad j=2,\ldots,N.$$

Passi attempts to estimate the improvement in wind accuracy with the spline over quadratic smoothing by comparing quadratic wind uncertanties (i.e., quadratic error predictions) with "actual" cubic spline errors estimated by tracking Omega upsondes with radar. He estimates that wind errors with the spline will be lower than the quadratic uncertainties by a factor of 3. He does not, however, compare spline errors with actual (rather than predicted) quadratic errors as this study does.

The idea of cubic spline smoothing is to use more information than that contained in any 3-min interval alone, allowing continuity of the wind field to influence the solution. The

cubic nature of the individual polynomials should allow this routine to handle aircraft maneuvers better than the quadratic, while the node restrictions should eliminate window effects. Another important benefit is that winds can be computed at all points along the drop down to the surface, making postprocessing with this wind-finder particularly attractive. It is possible, however, that wind accuracy near these exterior nodes would be low since there are no continuity restrictions at these points; certainly bad Omega would cause difficulties here. One might also wonder about the effect of the continuity restrictions on the wind-finder's resolution. These questions and others regarding the performance of the three routines are examined in section IV.

III. DATA

How shall we evaluate the accuracy of Omega wind estimates? In the normal use of ODW's, the winds are, of course, unknown. Predictions of wind-finding accuracy for particular regions have been made by Acheson (1974), Passi (1973), and others by modelling or ignoring some of the factors influencing accuracy. Attempts have also been made to compare ODW winds with winds derived from radar tracking of ascending sondes by Passi (1977), and by Julian (1982) using standard dropwindsondes. Such radar tracking also contains error, however, and the proper attribution of the differences between radar and Omega winds is unclear. This study is different in that Omega wind errors are measured directly by using motionless sondes. The effects of station-sonde geometry and different levels of interference are simulated by computing winds with many different station combinations and by using raw and edited Omega signals.

On 4 August 1982, and on 13 September 1983 the NOAA Research Facilities Center (RFC), (now Office of Aircraft Operations) flew missions in which Omega signals were received from stationary sondes that were resting on Key Largo and Virginia Key, Florida. During the first mission, the RFC aircraft flew "L" patterns (Fig. 1a) and received adequate Omega for wind-finding for about 95 min. The second mission's aircraft flew a triangular pattern (Fig. 1b) and collected usable Omega for about 50 min. Flight level for the missions was 790 mb for the first and 450 mb for the second, the latter being more typical of normal dropwindsonde missions.

Actual Omega wind errors in these cases are known directly; they are given by the computed wind speed, since true sonde velocity is zero. A second experiment during the first mission involved a sonde on a boat moving with a known but changing velocity; unfortunately, interference from the boat's motor prevented adequate signals from being received on the aircraft.

This experiment would have allowed an evaluation of the different wind-finders' ability to resolve wind shear. The question of resolution is addressed instead by applying each wind-finder to a time series of simulated Omega signals. The data collected by the RFC aircraft will primarily address the question of how each of several wind-finders react to noisy Omega and aircraft maneuvers.

As Omega signals were received during the flights, an on-board computer calculated winds for real-time inspection. The Omega signals were stored on cassettes for postprocessing at the HRD, where they could be displayed and examined for noise spikes and other problems that typically degrade the quality of real-time wind estimates. The original data set was then divided into two parts: one in which the Omega was left just as it had been recorded on board, and one in which the noise was subjectively removed. This Omega editing is standard procedure in dropwindsonde processing; it removes spurious winds often found in wind profiles that have been computed from raw Omega (Franklin, 1983). Figures 2 and 3 show examples of typical raw and edited Omega data from the 1982 flight. The rapid changes in slope identify the aircraft turns, which are labelled by letter corresponding to the turn points in Fig. 1a. Figure 4 shows a sample of raw Omega from the 1983 mission. The turns, which are not as obvious here because of the flight-track geometry, are marked by brackets and labeled according to their locations in Fig. 1b. Notice that the worst Omega reception tends to occur while the aircraft turns. This partial loss of signal is caused by "shadowing" of the Omega antenna. As the roll angle of the aircraft increases to execute a turn, the antenna (mounted on the underside of the plane) may find itself "behind" the aircraft relative to the sonde. This would temporarily reduce signal strength (Farr, 1983, private communication). As a result of shadowing, one would expect real-time Omega-derived wind accuracy to be low during turns. That winds computed using edited Omega would also

be less accurate during turns for some wind-finders has been suggested in section II and is demonstrated in section IV.

Editing decisions, while subjective, were based on experience with many other data sets, including ALPEX, El Nino, and Hurricane Debby. Because of the complexity of the wind-finding computation and its sensitive dependence on the slopes of the phase curves, it is extremely difficult, if not impossible, to produce a particular desired wind field through selective editing of Omega data. There should be no concern, therefore, that the edited data set has been biased to yield desired results.

After the substantial job of Omega editing had been completed, winds were computed for both raw and edited Omega using the three wind-finders described earlier. Software to compute winds using the quadratic and low-pass filter smoothers was already in place on the HRD HP-1000 minicomputer. The cubic spline wind solutions were obtained on the Environmental Research Laboratories' CDC-750 computer in Boulder, Colorado, and sent on magnetic tape to HRD for analysis. Results of these wind-finding efforts follow in section IV.

IV. RESULTS AND DISCUSSION

The basic data set for this study consists of raw (R) and edited (E) phases for each of the two research flights. These four subsets of phase data are abbreviated by 82R, 82E, 83R, and 83E. Of the eight Omega stations, six provided adequate signals for wind-finding during the 1982 flight, while only five were available for the 1983 mission. The eight stations, their locations, and those used for wind-finding are given in table 1. Figure 5 shows the station-sonde geometry for the two missions.

Omega winds are usually computed from as many Omega stations as are available (except in real-time, where no more than four may be used). So that the results of this study would be applicable to outside the south Florida area, winds in this study were computed using 12 station combinations in an attempt to simulate the geometries of other regions. These combinations were chosen to represent a range of possible geometries, from optimal to marginal. (Optimal geometry is obtained by maximizing the angular separation of the Omega stations while avoiding the use of antipodal stations; for example, the three-station combination of Hawaii, Norway, and Argentina is excellent.) Each of the three wind-finding algorithms was used with each combination for the four phase subsets, so that, in all, 144 wind time-series (profiles) were produced. For each of the 144 profiles, the following instantaneous quantities were calculated at 10-s intervals: the actual wind error (WE), which for these stationary sondes equals $\{U^2+V^2\}^{0.5}$, where U and V are given by (10); the estimated wind error, or wind uncertainty (WU), defined by $\{\text{Var } U + \text{Var } V\}^{0.5}$; and the wind error ratio R, defined to be WE/WU. $\bar{X}$ shall denotes the profile (time) average of the quantity X over either 95 or 50 min, depending on the flight. For example, $\bar{W}\bar{E}$(83R,QUAD,2345) refers to the mean wind error for the 1983 raw phase data, computed using the quadratic wind-finder with stations 2, 3, 4, and 5 (table 1). $\langle\bar{X}\rangle$ refers to an average

over all 12 station combinations of the time-mean of X, so that $\langle\overline{WU}\rangle$(82E,SPL) is the average wind uncertainty (over time and "geometry") for the cubic spline wind-finder for the edited 1982 phase subset.

We now begin our investigation into the performance of ODW's. This investigation is divided into two main parts; first, we examine ODW performance in aircraft maneuvers; then we look at a few more general features of the three wind-finders under scrutiny in this paper. There is some overlap in the discussion, which we hope the reader will find reinforcing rather than repetitive.

A. ODW Performance: Turns Versus Legs

One would suspect that raw Omega would be particularly susceptible to reduced accuracy in turns because of poorer signal reception at these times (Figs. 2-4). Since only the quadratic wind-finder is used on real-time raw phases in normal aircraft operations, the effect of aircraft maneuvers on ODW accuracy is described primarily in terms of the quadratic.

Figure 6 shows wind uncertainty WU (82E,QUAD,234578) plotted against time for a portion of the 1982 flight. During this time the RFC aircraft made four turns, identified by the dashed arrows. The impact of these maneuvers on WU is dramatic, as the wind uncertainty increases from about 1.2 m/s during periods of straight-line motion (legs) to well over 3 m/s in the neighborhood of each turn. Notice that the intervals of high uncertainty are much larger than the length of the turns (about 45 s). This is because a wind estimate for time T is obtained from a window of phase data (3-min long, in this case) which may include a turn even though T itself is part of a leg. A quantity X(T) is described as coming from a turn, then, not only if T is contained in a turn, but also if any portion of the phase window surrounding T contains a turn. For the quadratic

and cubic spline wind-finders, we define T to be part of the turn sample if T falls within 105 s of the center of an actual aircraft turn. For the 4-min low-pass filter this limit is 135 s. We shall see shortly that actual wind errors for the quadratic are as large when a turn falls at the edge of the phase window as when one occurs at the center.

A striking aspect of Fig. 6 is the double peak of WU for each turn. One wonders whether actual wind errors (WE) behave in the same fashion. To address this question, turn points are further stratified into three subgroups based on their location on the uncertainty curve and are referred to as edge, peak, and center points. The definitions of these groups are given in table 2 and the groups are indicated in Fig. 6.

Figure 7 shows, in addition to the wind uncertainty given in Fig. 6, the actual wind error WE(82E,QUAD,234578) for the same period of time. There is much more short-term variation in WE than WU; remember that WU is an estimate of the variance of the wind, which will change much less rapidly than the wind itself. Nonetheless, there does appear to be a correlation between the two curves. In particular, it appears that those episodes of largest WE lie in the turn regions. To test this, the entire 95-min sequence of WE(82E,QUAD,234578) (of which Fig. 7 is a portion) was examined and 30 local maxima of WE were identified. The criteria for this selection were somewhat loosely defined; any local maximum of WE that appeared to last for a minute or more and that "struck the eye" of the author was included. Those maxima that fell in the time period of Fig. 7 are indicated in the figure. These 30 maxima then were classified as occurring in a turn or leg, depending on whether the midpoint of the maxima was a turn or leg point as described in table 2. Of the 30 maxima, 25 (83%) occurred during turns, although turn points make up only 58% of the sample. When one assumes a binomial distribution on the fraction of maxima in turns, a 95% confidence interval on this fraction is found to

be (Ø.7Ø-Ø.96), an interval that does not include Ø.58. Wind error maxima, then, do not occur randomly, but are more likely to occur in turns. Remembering that this is an edited phase subset, we see that this behavior is not due at all to signal shadowing, but rather is due solely to the limitations of the quadratic model.

A similar analysis was done for 26 identifiable minima in WE, some of which are also identified in Fig. 7. Of the 26, 16 (62%) occurred in the turns, about what one would expect from a random distribution (58%). Thus we conclude that although periods of low wind error are as likely to occur in turns as in legs, periods of relatively high error are more likely to occur in turns.

There is a hint in Fig. 7 that turn edges (table 2) might be particularly susceptible to these maxima in WE. This was tested in two ways. In the 95-min sample, there were 32 distinct turn edges. Of these 32, a WE maximum fell in 11, while a minimum in WE occurred in only 4. If we consider only the 15 cases in which either a maximum or a minimum fell in a turn edge, this is not a random distribution at the 95% confidence level; that is, a turn edge is more likely to produce an error maximum than an error minimum. The same statement could not be made for turn peaks or centers, however, as there was no preference for maxima over minima in these regions. A second test for the preference of maxima for turn edges examined the distribution of maxima <u>within</u> turns. Observed numbers of maxima in edges, peaks, and centers were 11, 1Ø, and 4, respectively, with corresponding expected counts of 1Ø, 1Ø, and 5. The chi-square p-value of Ø.86 indicates no preferential distribution of WE maxima within the turns. Still, this nearly random distribution suggests that a turn at the edge of the 3-min quadratic smoothing window will degrade the winds at least as strongly as if the turn were in the center of the window (assuming that all WE maxima are of equal magnitude).

While the preceding analysis gives some idea of where the highest and lowest wind accuracy can be found, it is more useful to examine mean values of wind error and uncertainty for the different groups over the 95-min sample. Table 3 shows these and other quantities for the wind profile that we have been examining, (82E,QUAD,234578). The table gives two sample sizes for each group; the first of these is the actual count of points in the sample. One would not expect each of these to be an independent estimate, however, since the 19-point phase window producing the wind at time T contains 18 of the 19 points used to produce the wind at T+1Ø. Given a number of serially correlated data points, one can estimate an equivalent number of independent points (World Meteorological Organization, 1979). The sequence of values WE(82E,QUAD,234578) was evaluated for serial correlation using this method, with the result that the 579 correlated points were equivalent to an independent sample of 272 points. The independent sample size given in the table is obtained by multiplying the actual sample size by Ø.47 (272/579). That nearly every second wind estimate is independent with the quadratic algorithm is at first very surprising, but it simply indicates that winds from the quadratic wind-finder are extremely dependent on phase points at the edges of the 3-min window. Knowing this helps us to understand table 3; as a turn enters the phase window, wind errors immediately rise from 1.93 m/s to 2.49 m/s, and remain approximately the same as the turn moves through the window. Wind uncertainty, which depends on the mean residual of the least-squares quadratic fit and not on the relative location of those residuals, rises more slowly, so that wind errors will be relatively underpredicted by the uncertainties about 9Ø s before and after the turn or noise spike causing the increase in error. This behavior has particular implications for those trying to make a real-time interpretation of Omega winds as they are computed on board the aircraft.

The table indicates that wind error in turns is greater

than that in the legs, and this difference can be shown to be statistically significant. Using a modified t-test on the equivalence of the means 1.93 and 2.51 with no assumption on the variances, one finds that $\overline{WE}$ for legs is different from $\overline{WE}$ for turns with a p-value of less than Ø.Ø1. We conclude that wind error in turns is higher than that in legs. Again, it must be remembered that we are considering postprocessed data here, where signal qualities in and out of turns are equal; hence the poorer performance of the quadratic in turns is, in fact, a statement about the quadratic.

We now broaden our view by considering table 4, which presents $\overline{WE}$ and $\overline{WU}$ for the 144 wind profiles computed from the 1982 research flight. We will refer to this table many times; for now consider only the columns for the quadratic wind-finder. For every geometry, $\overline{WE}$ for turns is higher than $\overline{WE}$ for legs, both for edited and raw Omega. When we average over geometry as well as time, $\langle\overline{WE}\rangle$ for turns exceeds $\langle\overline{WE}\rangle$ for legs by 25% (3.67 versus 2.93) for edited Omega, while for raw Omega this increase in error is 53% (5.14 versus 3.37). This reduced error difference for edited Omega reflects the correction of low signal quality experienced during shadowing as discussed in section III. In practical terms, avoidance of aircraft maneuvers is less important for those experiments in which real-time winds are unimportant and postprocessing of the phase data is planned.

Phase editing is one way to improve wind accuracy in turns; another way is to use a different wind-finder in the postprocessing. Looking at the cubic spline columns of Table 4, one sees that the spline seems not to be influenced by the presence or absence of turns; in fact, in the mean, errors for turns are slightly lower than those in the legs. Values for $\langle\overline{WE}\rangle$(82E,SPL) are 2.Ø2 and 2.13 for turns and legs, respectively. In the "best case" of (82E,SPL,234578), $\overline{WE}$ for turns and legs are 1.4Ø and 1.39. The low-pass filter routine gives a 26% increase in mean wind error for turns for the best-case profile (82E,FIL,234578) (2.31

versus 1.83, with a p-value on the equality of the means of Ø.13). The spline, then, is the only algorithm (of the three studied here) in which wind accuracy is not reduced in turns. There are probably two reasons for this behavior. A cubic fit to phase data does not imply a constant component of acceleration towards the Omega stations (as a quadratic does), a restriction not satisfied when the aircraft turns. Thus a cubic fit is better able to "handle" the sharp changes in phase slope shown in Figs. 2-4. Another factor, though, may be the continuity restrictions of the spline, in which phase data minutes away affect a wind estimate. These restrictions would tend to blur the distinction between turns and legs. It may still be true that spline winds are less accurate when turns are in the flight pattern, although the data collected for this study will not help to answer this question.

When we compare turn accuracy of the spline to the two other algorithms we find significant, but, by now, expected differences. For best-case geometry (82E,234578), mean error for the spline is only 1.4Ø m/s as noted above, compared with 2.31 and 2.51 m/s for the filter and quadratic (table 4). A modified t-test on the equality of these means gives p-values of less than .Ø1 for both the quadratic and the filter smoothers, so that the 4Ø% error reduction by the spline over the other methods represents a significant difference. This percentage reduction remains approximately the same when averaged over geometry.

Table 5 contains the results of the 1983 mission in the same format as table 4. One sees immediately that the overall level of wind accuracy is much lower for this second flight. The stations selected for wind computations for this data are not the same because of the lack of Hawaii's signal during the second flight, which accounts, in part, for the higher average wind error. Poorer quality Omega was also present, however, as station combinations common to both missions ([2378], [257],

and [278]) had lower errors for the first flight.

Despite the overall reduced accuracy, the trends observed in the 1982 data set are confirmed in the newer data. For the quadratic wind-finder, $\langle\overline{WE}\rangle$ for turns exceeds $\langle\overline{WE}\rangle$ for legs by 32% (6.87 versus 5.21) for edited data and by 48% (8.44 versus 5.71) for raw Omega, not far from the 1982 values of 25% and 53%, respectively. Spline wind accuracy is again lower in the turns than in the legs, but this time by substantial amounts (3.35 versus 4.31 for $\langle\overline{WE}\rangle$[SPL,83E]). The cause of this curious behavior is not at all clear; perhaps the relatively high-order spline is reacting to noise in the legs portions, while in the turns the cubic must primarily respond to the naturally large changes in phase slope present there. The analysis, complicated enough by the continuity restrictions of the spline, is further muddled by a flight track that removes phase-slope sign changes from turns and places them in legs (Fig. 4). In any event, it is clear that the spline has again outperformed the other algorithms in turns, with edited Omega geometric-mean wind errors of 3.35, 6.33, and 6.87 m/s for the spline, filter and quadratic. This is roughly a 50% reduction in error for the spline, about the same as the 40% reduction obtained with the 1982 data. The data from both flights clearly dictate that the spline should be the wind-finder of choice when turns are an important part of the flight track. We will see below that the spline should be used irrespective of the presence of turns.

B. Omega Wind-finding Algorithms

We now move to a more general comparison of the three wind-finders used in this study: quadratic smoothing, low-pass filtering, and cubic-spline smoothing of the Omega signals. The emphasis here is on performance during straight-line motion of the launching aircraft (legs) since, by far, most phase data

are collected during such motion, and performance during turns has already been discussed in section A.

B.1 Which Algorithm Is Best?

Figure 8 shows wind error and uncertainty for a portion of the (82E,234578) wind profiles for each algorithm. When used on identical phases, the three methods give profiles that vary greatly in smoothness. The quadratic, with its high dependence on window end points, varies most rapidly. The reduced uncertainty in the center of each turn implies that a second-order polynomial fits a turn with lower residuals when the turn is centered on the smoothing interval. Although the figure suggests that actual error may also be reduced at the turn center, table 3 reveals that, in the mean, this is not the case. The plot of WE for the filtered phases looks much like a highly smoothed version of the quadratic. The cubic-spline profile looks nothing like the other two, however, with slowly changing errors and uncertainties that bear little or no relationship to the turns. This dissimilarity is reflected in nearly identical turn and leg mean wind errors for this spline profile (1.40 and 1.39 m/s; see table 4).

These scales of variablility are reflected in the calculations of independent sample size for the three wind-finders. Recall (section A) that the sample size for quadratic wind estimates had to be reduced by only a factor of 2 to account for the serial dependence of the wind estimates. Similar calculations for the spline and the filter methods gave very different results. For the low-pass filter, an equivalent independent sample size was found to be 16% of the full sample, while, for the spline, this fraction was only 11%. This outcome is not surprising, since both the filter and spline allow all points even minutes away to influence wind solutions, while quadratic winds are primarily determined by a few points at the edges of the 3-min window.

We return to table 4, to determine whether one of the wind-finders is significantly better than the others. Looking at the left hand side of the table (legs), we see that for both raw and edited Omega the cubic spline gives the lowest errors. For best case edited signals, spline mean error is 24% lower than the low-pass filter and 28% lower than the quadratic, with means of 1.39, 1.83 and 1.93 m/s respectively. The modified t-test on the equality of the filter and spline means gives a p-value of Ø.15, a value not statistically significant due to the small independent sample sizes, but suggestive nonetheless. For the quadratic and spline means, the p-value is lower at Ø.Ø1. When we average over geometry, we find the spline maintains its leadership, with errors 19% and 27% lower than the filter and quadratic. The cubic spline has the lowest mean wind error of the three algorithms in 23 of the 24 "contests" on the left-hand side of table 4. Although statistical significance is not quite achieved over both competitors, it should be reasonably clear that the spline is the superior method, especially when its great success with turns is considered.

Data from the 1983 flight also indicate that the spline is the most accurate algorithm. Values of $\langle\overline{WE}\rangle$(83E) for the spline, filter, and quadratic are 4.31, 5.12, and 5.21 m/s; this is an error reduction of 16% over the filter and 18% over the quadratic. The spline has the lowest sonde-mean wind error for every case in table 5; for turns and legs, for raw and edited signals, and for every station combination, the smallest errors come from the spline.

Note that although the spline algorithm permits the calculation of winds from the first phase point to the last, winds computed in the first and last 9Ø s of each profile were not included in any of the means in tables 4 and 5. This was done to keep the samples for the three methods equivalent. As one would expect, wind accuracy at the edges of the spline is not as high as in the interior. For the case of WE(82E,SPL,234578),

wind error in these edges is 2.50 m/s, compared with 1.39 m/s for the remainder of the profile (table 4). A subjective examination of these edges for other station combinations shows examples of varying wind accuracy in these regions. Until this effect has been investigated in greater detail, much care should be taken in the interpretation of spline winds at the beginning and end of drops.

Although the spline has been shown to be more accurate than the quadratic or filter for the two stationary sondes, one might be concerned about the resolution of the spline, and hence, its suitability for soundings with significant wind shear. To examine the question of resolution, a time series of simulated Omega signals was created. Using (8), noise-free phase rates corresponding to selected values of U and V were computed to form a 20-min "synthetic" sounding. For simplicity, phases were created for only three Omega stations (Norway, North Dakota and Argentina). The winds used in the synthetic sounding were taken from rawinsonde data for Dodge City, Kansas at 0 GMT on December 6, 1978, and feature a distinct frontal zone with a wind shear of 2.4×10^{-2} s^{-1} between 725 and 750 mb (fig. 9). A wind shear of similar magnitude is also observed near 650 mb. "Truth" values of U and V at 20 s (about 10 mb) intervals were obtained by interpolating between the points in Fig. 9. Synthetic phase data were computed using these interpolated winds in (8), and the synthetic phases were then used to estimate winds with the three wind-finders.

Wind errors for the three wind-finders are shown in Fig. 9. Errors for all three wind-finders increase dramatically in the frontal zone; none of the algorithms can accurately resolve such a wind shift. Wind errors are also large above the frontal zone in the second region of highest shear. Over most of the sounding, however, errors are generally less than 2 m/s.

The spline is clearly the weakest of the three wind-finder in terms of wind-shear resolution. Average error for the spline

with this sounding is 1.72 m/s, compared with average errors of 1.Ø1 and Ø.89 m/s for the filter and quadratic algorithms. In the two regions of highest shear, the spline has by far the highest errors, and below the frontal zone, a brief veering of the wind to the northeast is picked up by the quadratic and filter, but not by the spline.

One must be very careful in drawing conclusions from this experiment. The poor performance of the spline in resolving the fine structure of the wind field does not imply that the quadratic or filter algorithms would yield more accurate winds in a real sounding. The continuity restrictions at the nodal points of the spline, which are responsible for its relative lack of resolution, are also responsible for the spline's ability to extract accurate phase rates from real (i.e., noisy) Omega (as demonstrated by the stationary sonde experiments). There is a trade-off between resolving power and sensitivity to noise. Through its continuity restrictions, the spline increases its effective sample of phase points for the cubic fit, reducing phase variance and the effects of noise, but in doing so it ignores "local" changes in phase rate that represent regions of high shear. The quadratic, on the other hand, examines only three minutes of data at a time. This makes the quadratic more responsive to smaller-scale changes in phase rate, but also makes it highly susceptible to unrepresentative phase measurements. The current accuracy of Omega phase measurement dictates that wind-finding algorithms must primarily be able to handle noise. This can be demonstrated by adding artificial noise to the synthetic sounding. For simplicity, a random "error" having a uniform distribution over (-2,+2 cec) was added to each synthetic phase value. This produced phase time series with variances (given by (12)) of about 1.5 cec^2. This is approximately the level of noise found in real Omega signals of high quality, which rarely have variances less than 1.Ø cec^2 (Passi, 1977). When these phase errors were added to the synthetic sounding,

mean wind error with the quadratic increased 135%, from 0.89 to 2.09 m/s. With the spline, however, mean error only increased 17%, from 1.72 to 2.02 m/s. Even though this model for noise is quite simple, it seems reasonable to conclude that the quadratic's high resolution is a liability, not an asset, for all but the cleanest Omega signals.

The low-pass filter was virtually unaffected by the addition of noise; wind errors increased from 1.01 to 1.05 m/s. This is not surprising since uncorrelated random noise is the precise target of the low-pass filter. Tables 4 and 5, however, show that improvements in wind accuracy due to phase editing are larger with the filter than with either the quadratic or spline. This relatively strong filter dependence on real-world phase errors suggests that the noise model described above is unrealistic, or that other relevant factors are not being taken into account. Correlated phase errors, not modeled above, would survive filtering and reduce wind accuracy; Govind (1975) describes one way in which atmospheric noise could produce such errors in Omega phases. The effect on wind estimates of small but ever-present variations in aircraft velocity is another possibility.

Which windfinder, then, should we recommend for use in ODW postprocessing? When flight tracks involve turns, it is clear that the cubic spline can provide the most accurate wind estimates. In cases where there are no turns, however, the choice is not as clear. The low-pass filter has the advantages of relatively high resolution and insensitivity to uncorrelated random noise; however, it is difficult to recommend this method until its high accuracy with synthetic soundings can be more fully reconciled with its poorer performance with the stationary sondes. The 60-70 mb layers after launch and before splash, during which no winds are estimated, also make this algorithm less desireable than the other methods. In cases of very low phase variance (about 1.0 cec^2), the quadratic should be considered if maximum resolution is desired. For noise levels typically found in

real-world Omega data, however, the synthetic and stationary sonde experiments suggest that the spline will give more accurate wind estimates, despite its lower resolution. It has the additional advantage of providing wind estimates immediately after launch and before splash. We recommend, then, that cubic spline smoothing be used for most ODW postprocessing.

B.2 The Value of Wind Uncertainties

Wind uncertainties (WU) or estimated wind errors, can be computed easily as part of the wind-finding procedure. They depend upon two factors only: the quality of the sonde-station geometry, and the quality of the fit of the smoothed phases to the original phase data. They cannot take into account factors that are external to the dropwindsonde system, such as unsteady or anomalous propagation of the Omega signals. Figure 8 hints that uncertainties are, at best, indicators of mean wind accuracy over some period of time and are probably not useful predictors of actual wind error on an instantaneous basis.

Figures 10-12 are scatter diagrams of WU versus WE for every 10-s wind calculation of (82E,234578) using the three wind-finders. Correlation coefficients have not been calculated for these cases, but they are certainly very small; it is clear that knowledge of the wind uncertainty at a given point indicates almost nothing about the actual wind error at that point. A possible use for uncertainties on a point-by-point basis would be as identifiers of turns and noise spikes (with the quadratic and filter algorithms) that might be accompanied by increased error, although it is apparant that high WU is neither a necessary nor sufficient condition for high WE.

If one averages WE and WU over the length of each wind profile (tables 4 and 5), their behavior becomes more regular. The sonde-mean WE-WU pairs listed in these two tables are plotted in Figs. 13 and 14 (for the legs only). Notice first that the

best profiles (those in the lower left of the figures) are produced by the cubic spline. Notice also that, for the raw phases of both research flights, fitted curves relating mean WE to mean WU would be nearly identical for the three wind-finding algorithms. This is a satisfying observation, since the uncertainties for these algorithms were scaled by different investigators with different test drops (Passi, 1977; Julian, 1983, private communication). The clustering of points close to the $\overline{WE}$-$\overline{WU}$ line is also satisfying, since it indicates that the wind uncertainties have been scaled fairly accurately. Winds computed from edited data behave differently, however. The heavily edited data from the 1982 flight show a division on the basis of algorithm, indicating that, at least for this data set, editing has had different effects on the three smoothing methods. Examination of table 4 and Fig. 13 reveals that editing has little effect with the cubic spline, while its primary effect with the quadratic is to reduce uncertainty and with the filter to reduce actual error. A second separation can be seen in the edited 1983 data, as the spline profiles lie above and to the left of the others (Fig. 14). Table 5 reveals that spline wind profiles have become <u>less</u> accurate after phase editing. The reason for this behavior is not clear but the lesson to be learned is; namely, one should not edit noisy Omega signals when the spline will be used to estimate the winds.

One feature of Fig. 13 is the nonlinearity of the $\overline{WE}$-$\overline{WU}$ relationship; i.e., the slope of this relationship is close to one for low uncertainty, but appears to approach zero as the uncertainty increases. This behavior is displayed somewhat differently in Fig. 15. In this figure, for the 12 wind profiles (82E,QUAD), each 1Ø-s wind measurement is assigned to a class on the basis of its value of WU and whether it is a turn or leg point. For example, all winds from the leg portions of (82E,QUAD,247) with uncertainties between 1 and 2 m/s are represented by one point in Fig. 13. The means of WU and R=WE/WU

for each class containing at least 15 points are plotted in the figure. One hopes that R will be approximately 1.0 for the range of uncertainties, but this is not the case. Low uncertainties are seen to be substantial underestimates of actual error, while high uncertainties tend to slightly overestimate the wind errors. This is not a behavior peculiar to the quadratic, as Fig. 16 shows a similar trend with the cubic spline. Some of this change in the value of R, at least in the case of the quadratic, seems to be due to editing. Figure 17 is the raw-Omega counterpart to Fig. 15, and although the dependence of R on uncertaintty is reduced, there remains a behavior that cannot be explained by "human" interference.

Why the error ratio R should depend upon the magnitude of the uncertainty is difficult to explain. Recall that uncertainty measures error that is due only to the effects of geometry and signal quality. Actual wind errors can be due to other causes as well (WE can be expressed as WU + X, where X represents errors external to the uncertainty calculation). One is thus tempted to speculate that other sources of error may become evident when uncertainties are low. These errors would be small compared to the typical errors due to noisy Omega and poor geometry. Two possible sources of such error are the diurnal effects of signal transmission through sunrise or sunset, and sudden ionospheric disturbances that temporarily alter the path of signal propagation (Acheson, 1974). The diurnal effects are modeled by the wind-finders in this study, albeit crudely, and are probably not having a noticeable influence on the computed winds. If it is true that a propagation phenomenon is responsible for the behavior of the error ratio, Acheson showed remarkable insight when he suggested that "as the...noise problem diminishes with the use of high-power VLF transmitters, problems with propagation we have previously been able to ignore as being relatively small will likely become the more important [and] set the limit on windfinding performance".

C. The Effect of Post-Processing

The data presented in this study demonstrate clearly that wind accuracy from Omega dropwinsondes can be significantly improved by reprocessing with the cubic-spline wind-finder. The on-board quadratic algorithm has two major deficiencies that degrade the quality of real-time winds: the quadratic model is inappropriate for aircraft maneuvers, and it is very sensitive to noisy Omega on the edges of its 3-min smoothing window. By using the low-pass filter algorithm on many soundings and by editing poor Omega, Franklin (1983) observed changes in direction of at least 20 degrees or in speed of at least 5 m/s in 29% of the standard level wind reports for the HRD flights around Hurricane Debby. With data from our stationary sondes we can estimate the improvements to be expected from postprocessing by comparing wind errors from the quadratic using raw Omega with those from the spline using edited Omega. From table 4 we see that in the geometric mean, postprocessing reduced mean wind error by 37% in the legs (3.37 to 2.13 m/s) and by 57% in the turns (5.14 to 2.02 m/s). For the individual geometries, error reductions ranged from 14% to 47% in the legs and from 52% to 67% in the turns. The overall poorer signal quality and geometry of the 1983 data given in table 5 do not seem to affect these error reductions greatly; geometric-mean error reductions for the 1983 flight are 25% and 60% for legs and turns, respectively. These would seem to be significant reductions in wind error for nearly all meteorological applications.

The error reductions quoted above all consider only the effects of editing noisy Omega and the use of the cubic-spline smoother. Examination of tables 4 and 5 shows that further improvements in accuracy can be obtained by adding a fifth or sixth Omega signal to the postprocessed wind computation (recall that no more than four may be used in real-time). $\overline{WE}$(82E,SPL) averaged over the four-station combinations is 1.83 m/s, compared

with 1.42 and 1.39 m/s for the five and six-station combinations, respectively. There are similar reductions in the 1983 data. This additional 20-25% reduction in error through postprocessing would not occur in all cases, however. If the four stations selected in real-time were nearly optimal, the reduction of error obtained by using additional stations would be small. Furthermore, many times only three or four usable Omega signals are available. Nonetheless, in most cases the inclusion of a (generally available) fifth station should result in an additional error reduction of 10-20%.

V. SUMMARY AND CONCLUSIONS

It was observed that aircraft turns greatly affect the accuracy of real-time wind estimates; that is, winds estimated with the on-board quadratic wind-finder using raw Omega. In the geometric mean, wind error during turns was 51% higher than in legs for the two flights. About half of this increase was due to the shadowing of the Omega antenna during turns, with the remainder due to the quadratic's implied assumption of constant aircraft acceleration.

Of the three wind-finders investigated in this study, the cubic-spline phase smoother clearly outperformed both the quadratic and low-pass filter methods on the stationary sonde data of both research flights. In turns, using edited Omega signals, wind errors for the spline averaged 48% lower than the quadratic and 43% lower than the low-pass filter. These are average figures over many Omega-station combinations that represent all qualities of station-sonde geometry. For soundings with turns, then, the spline is the recommended wind-finder for ODW postprocessing.

During periods of straight-line aircraft motion (legs), stationary sonde wind errors with the spline were lower than those of the quadratic and filter by 22% and 18%, respectively, for high-quality edited Omega, and by 34% and 33% for the noisier raw phases. Results of the synthetic sounding experiments indicated that the quadratic had the finest resolution of the three methods, although phase variances of 1.Ø cec^2 or less, as well as an absence of turns, are necessary to take advantage of this higher resolution. Most Omega signals, even after editing, contain sufficient noise to warrant use of another wind-finder. The low-pass filter performed extremely well with the synthetic soundings, but questions remain concerning its accuracy with real-world Omega. We therefore recommend the cubic spline wind-finder for <u>all</u> ODW's containing typical amounts of noise.

An estimate of the effect of postprocessing was made by comparing wind error with the quadratic using raw Omega against error with the spline using edited Omega. The postprocessed wind errors averaged 31% lower than real-time errors in the legs and 59% lower in the turns. Thus, highly significant reductions in wind error can be expected through postprocessing.

Results of this study indicated that wind uncertainties (predicted wind errors) had been scaled accurately by previous investigators. Sonde-mean uncertainties were useful in estimating the mean wind error in a sounding, but instantaneous uncertainty estimates bore little relation to actual errors and probably should be replaced by the sonde-means in future postprocessed data sets (particularly if the spline wind-finder is used).

Finally, although very low uncertainties were observed in this study (<1 m/s), actual wind errors did not drop as low as the uncertainties. This suggests that sources of error external to the uncertainty calculation (such as ionospheric disturbances) may produce noticeable effects when other errors become small. If this is true, we may be approaching a practical lower limit on Omega wind error, which neither perfect geometry nor noise-free signals could overcome. Fortunately, such a lower limit would probably be small; sonde-mean wind accuracies of 1.3 m/s were achieved for the test drops of this study.

Although much has been learned about Omega wind accuracy and the three phase-smoothing algorithms, many questions still remain. The true effect of turns on cubic spline winds is hard to gauge with only one flight track, since the classification of "turn" and "leg" points may be meaningless in light of the spline's continuity restrictions. A one-sonde, two-aircraft experiment in which only one plane executes turns would address this question but only at high cost. A more economical alternative would be to add "aircraft" motion to existing synthetic soundings. More work with such soundings could also increase our understanding of the filter's performance with the stationary sonde data.

With the data already collected, however, progress could be made in the problem of wind accuracy at the ends of the spline. Any of a number of restrictions can be made at the end points; these restrictions should be investigated so that surface wind estimates can be obtained with greater reliability. Perhaps the most intriguing questions raised by this research, however, are those concerning the high error ratios for low wind uncertainties. The causes of this behavior, and the variablility of this apparent lower limit on Omega wind accuracy, as well as the other questions raised above, should be points of future investigation.

ACKNOWLEDGMENTS

The author wishes to thank the people at NOAA/RFC, particularly Jim DuGranrut, for their interest, skill, and cooperation in the design and execution of the field experiments. The author is indebted to Dr. Paul Julian of NCAR for the helpful consultations and guidance he provided during this research, and for the cubic-spline wind-finder FORTRAN code. Thanks are also due Joe Griffin (HRD) for his time in the computation of the cubic-spline winds. The flexibility and understanding of Professors Frederick Sanders and Richard Passarelli of MIT regarding the topic of this research are greatly appreciated. A very special thanks is extended to Dr. Robert Burpee of HRD; his constant encouragement and support contributed immeasurably to the completion of this paper.

REFERENCES

Acheson, Donald T., 1974: Omega windfinding and GATE. Bull. Amer. Meteorol. Soc., 55, 385-398.

Franklin, James L., 1983: Omega dropwindsonde processing. NOAA Tech. Memo. ERL AOML-54, 34 pp.

Govind, P. K., 1975: Omega windfinding systems. J. Appl. Meteorol., 14, 1503-1511.

Julian, Paul R., 1982: The aircraft dropwindsonde system in the global weather experiment. Bull. Amer. Meteorol. Soc., 73, 619-627.

Passi, Ranjit M., 1973: Errors in wind measurements derived from Omega signals. NCAR Tech. Note TN/STR-88, 35 pp.

———, 1974: Wind determination using Omega signals. J. Appl. Meteorol., 13, 934-939.

———, 1977: Smoothing improvement factor in Omega errors. J. Appl. Meteorol., 16, 735-739.

World Meteorological Organization, 1979: Operational techniques for forecasting tropical cylone intensity and movement. WMO-No. 528, Geneva, Switzerland.

Table 1. The locations of the eight Omega transmitters. The stations used for windfinding have been identified with an "x".

Number	Station Name	Latitude	Longitude	Used 1982?	Used 1983?
1	Japan	34.6 N	129.4 E		
2	Norway	66.4 N	13.2 E	x	x
3	Liberia	6.3 N	10.7 W	x	x
4	Hawaii	21.4 N	157.8 W	x	
5	N. Dakota	46.4 N	98.3 W	x	x
6	La Reunion	21.0 S	55.3 E		
7	Argentina	43.0 S	65.1 W	x	x
8	Australia	38.4 S	147.0 E	x	x

Table 2. Stratification of sample. Classification of a wind estimate valid at time T is determined by the value of $D=|T-\tau|$, where τ is the time of the midpoint of the nearest aircraft turn. Units for D are seconds.

	Quadratic	Low-pass Filter	Cubic-spline
Leg	D>105	D>135	D>105
Edge	65<D<105	105<D<135	65<D<105
Peak	25<D<65	35<D<105	25<D<65
Center	D<25	D<35	D<25
Turn	D<105	D<135	D<105

Table 3. Error Statistics for (82E,QUAD,234578)

	Sample Size	Independent Sample Size	$\overline{WE}$ (m/s)	$\overline{WU}$ (m/s)	$\overline{R}$
Legs	228	107	1.93	1.19	1.63
Turns	351	165	2.51	2.65	1.06
Edges	136	64	2.49	1.98	1.39
Peaks	140	66	2.44	3.29	0.75
Centers	75	35	2.66	2.69	1.01

Table 4. Sonde-mean wind errors and wind uncertainties for 1982 research flight. Wind error is given first, all values are in m/s.

	LEGS						TURNS					
	EDITED OMEGA			RAW OMEGA			EDITED OMEGA			RAW OMEGA		
STATIONS	QUAD	FILTER	SPLINE	QUAD	FILTER	SPLINE	QUAD	FILTER	SPLINE	QUAD	FILTER	SPLINE
234578	1.93 1.19	1.83 1.94	1.39 0.95	2.02 1.55	2.27 1.99	1.31 0.95	2.51 2.65	2.31 3.42	1.40 1.07	2.91 3.64	2.71 4.29	1.30 1.12
23457	1.99 1.35	1.89 2.22	1.42 1.11	2.15 1.78	2.57 2.29	1.63 1.10	2.39 3.02	2.14 3.88	1.46 1.22	3.39 4.19	3.27 4.95	1.42 1.22
2347	2.25 1.59	2.14 2.49	1.56 1.32	2.77 2.53	2.80 2.64	1.67 1.30	2.62 3.33	2.31 4.25	1.51 1.45	3.90 4.78	3.71 5.54	1.46 1.46
2457	2.29 1.67	2.23 2.71	1.64 1.57	2.50 2.14	2.79 2.86	2.01 1.52	2.69 3.66	2.51 4.68	1.60 1.76	4.06 5.11	3.84 6.00	1.67 1.76
2345	2.59 1.97	2.53 3.35	2.15 1.92	2.71 2.57	3.06 3.62	2.06 2.00	3.34 4.60	3.22 5.94	1.94 1.98	4.01 6.38	3.87 7.62	1.83 2.15
2378	2.98 1.82	2.55 2.73	1.96 1.39	3.55 2.55	3.48 2.97	2.09 1.39	3.48 3.58	3.22 4.65	1.98 1.55	4.87 5.47	4.69 6.19	1.94 1.65
247	2.55 1.86	2.40 2.94	1.63 1.68	2.98 2.43	3.01 3.37	2.01 1.64	2.87 3.92	2.61 4.99	1.61 1.89	4.78 5.78	4.39 6.66	1.67 1.91
257	2.99 2.39	2.55 4.00	2.33 2.36	4.04 4.26	3.42 4.59	2.41 2.29	3.68 5.43	3.19 6.98	2.16 2.74	6.04 8.37	5.58 9.71	2.05 2.79
245	3.48 4.74	2.62 8.79	3.26 5.12	3.80 6.55	3.64 9.92	3.06 5.25	5.40 12.68	4.35 16.45	2.99 5.25	6.21 16.63	5.61 19.39	2.79 5.41
234	3.61 2.66	3.23 4.10	2.73 2.53	4.05 4.02	3.77 4.74	2.40 2.65	4.24 5.34	3.95 6.78	2.34 2.73	6.24 8.66	5.67 9.95	2.28 3.12
278	3.51 2.35	3.01 3.48	2.29 1.95	4.35 3.41	3.81 3.92	2.47 1.94	4.40 4.59	4.10 5.77	2.26 2.14	6.00 7.00	5.56 7.72	2.27 2.21
458	4.95 5.63	4.42 9.54	3.15 5.57	5.56 7.52	5.85 10.09	4.37 5.41	6.38 13.12	5.53 16.88	3.04 6.78	9.24 17.17	8.61 19.46	3.63 6.50
<WE> <WU>	2.93 2.44	2.62 4.02	2.13 2.29	3.37 3.44	3.37 4.42	2.29 2.29	3.67 5.49	3.29 7.06	2.02 2.55	5.14 7.77	4.79 8.96	2.03 2.61

Table 5. Sonde-mean wind errors and wind uncertainties for 1983 research flight. Wind error is given first, all values are in m/s.

	LEGS						TURNS					
	EDITED OMEGA			RAW OMEGA			EDITED OMEGA			RAW OMEGA		
STATIONS	QUAD	FILTER	SPLINE	QUAD	FILTER	SPLINE	QUAD	FILTER	SPLINE	QUAD	FILTER	SPLINE
23578	3.69 2.73	3.81 2.86	2.76 1.12	3.86 3.18	4.10 2.76	2.58 1.13	4.00 3.30	3.70 3.67	2.22 1.10	5.14 4.64	4.79 4.93	2.33 1.22
2578	4.28 3.52	3.93 3.66	3.34 1.49	4.68 4.08	4.52 3.54	3.26 1.45	5.48 4.41	4.91 4.82	2.44 1.53	6.12 6.17	5.63 6.36	2.76 1.64
2378	4.18 3.87	4.09 4.05	4.03 1.50	4.22 4.65	4.03 4.00	3.61 1.51	5.90 4.51	5.26 4.91	3.00 1.55	6.27 6.62	5.51 6.75	2.94 1.69
2358	4.34 3.31	4.33 3.46	2.77 1.44	4.74 3.90	4.93 3.51	2.59 1.44	5.07 4.04	4.76 4.51	2.19 1.53	6.14 5.44	5.67 5.87	2.32 1.62
2357	4.17 3.64	4.71 3.91	3.55 1.70	4.62 4.42	5.35 3.68	3.35 1.71	4.87 4.32	4.53 4.76	2.68 1.86	6.49 6.79	6.09 6.72	2.72 1.65
357	4.84 5.26	5.35 6.17	4.14 2.23	5.36 7.74	5.53 6.34	3.25 2.30	7.06 5.80	6.22 6.28	3.57 2.70	8.46 9.54	7.27 9.75	3.32 2.33
278	4.77 4.68	4.14 4.85	3.98 2.07	5.05 5.72	4.37 5.27	3.56 2.03	7.60 6.04	6.59 6.43	3.27 2.40	7.39 8.98	6.52 8.65	3.42 2.49
237	7.10 7.55	7.16 8.28	6.34 3.24	8.21 9.70	7.46 8.34	4.75 3.36	10.84 8.12	9.89 9.02	5.51 3.92	14.83 12.90	11.80 13.18	4.98 3.48
238	5.49 5.87	5.10 6.32	4.89 2.17	6.00 7.28	5.98 6.30	4.15 2.19	8.04 6.15	7.69 6.91	3.85 2.56	10.39 9.34	9.20 9.98	3.62 2.77
358	4.83 3.66	4.94 3.89	3.30 1.73	5.12 4.56	5.07 4.14	2.96 1.70	5.59 4.53	5.32 5.10	2.57 2.05	6.60 6.03	5.86 6.53	2.57 2.11
235	8.94 10.68	8.05 10.22	7.57 4.90	10.20 12.45	8.27 10.25	7.77 5.20	11.75 11.87	10.97 12.83	5.64 5.50	15.52 15.21	14.06 16.91	5.89 5.97
257	5.90 5.00	5.87 5.44	5.07 2.48	6.41 5.68	6.86 5.04	5.48 2.45	6.20 5.97	6.12 6.54	3.20 2.76	8.37 8.78	8.51 9.05	3.74 2.30
<WE> <WU>	5.21 4.98	5.12 5.26	4.31 2.17	5.71 6.11	5.54 5.26	3.94 2.21	6.87 5.76	6.33 6.32	3.35 2.46	8.44 8.37	7.58 8.72	3.38 2.44

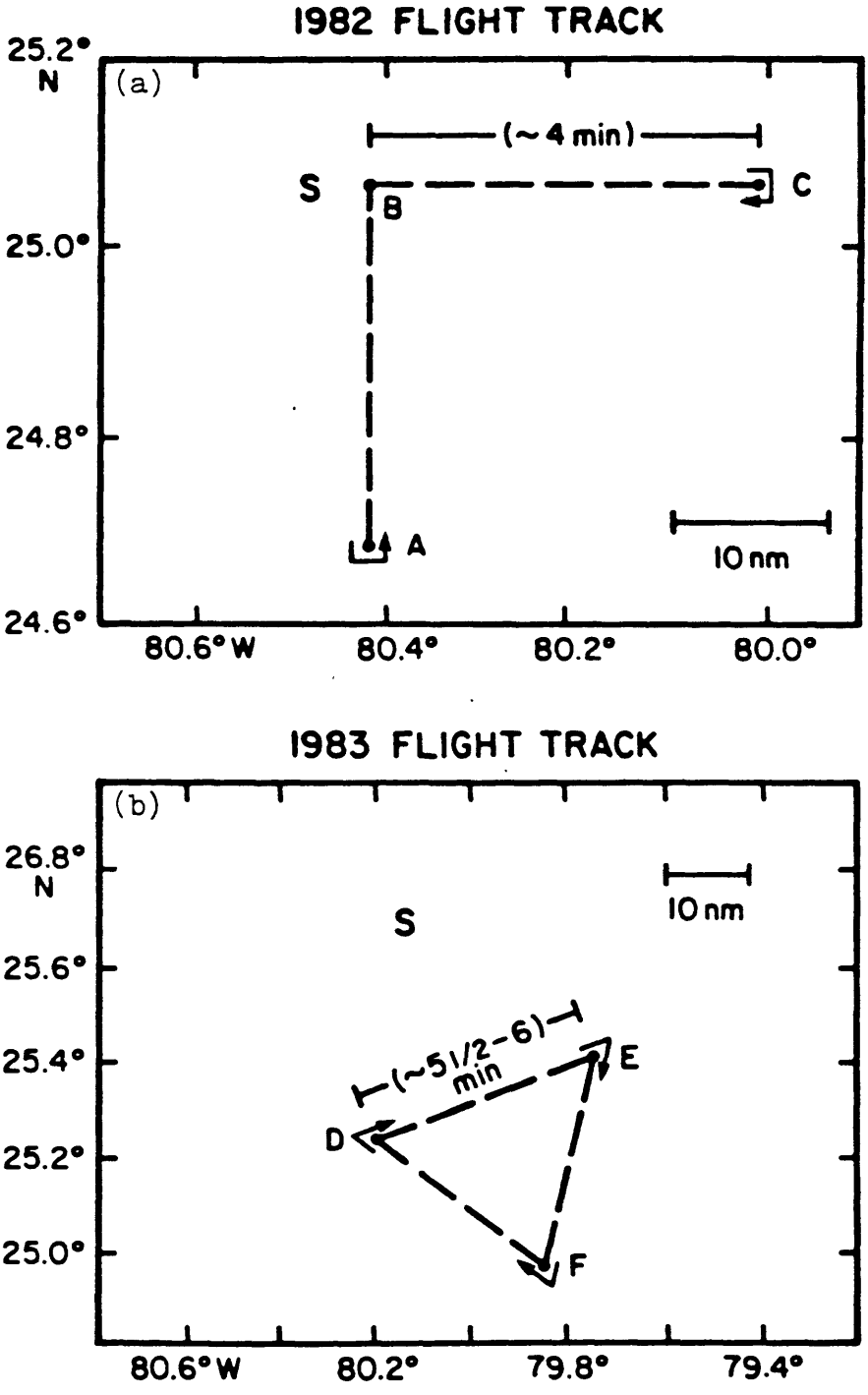

Figure 1. Flight tracks for the missions of 4 August 1982 (a) and 13 September 1983 (b). Position of the sonde is marked by the "S." Turn types are identified by letter.

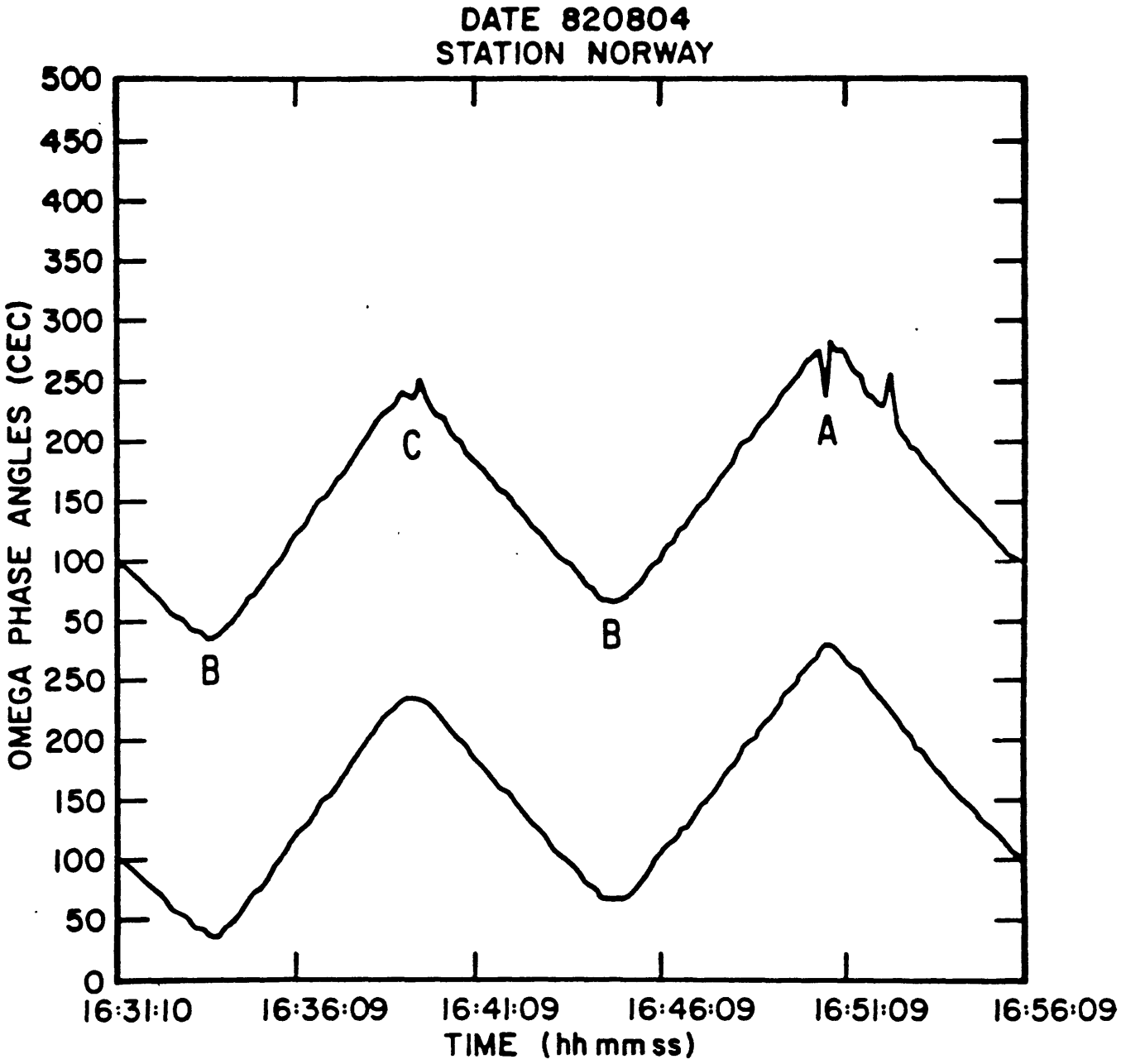

Figure 2. Raw (top) and edited (bottom) Omega signals from the Norway station during part of the 1982 mission. Turn labeling corresponds to that in figure 1a.

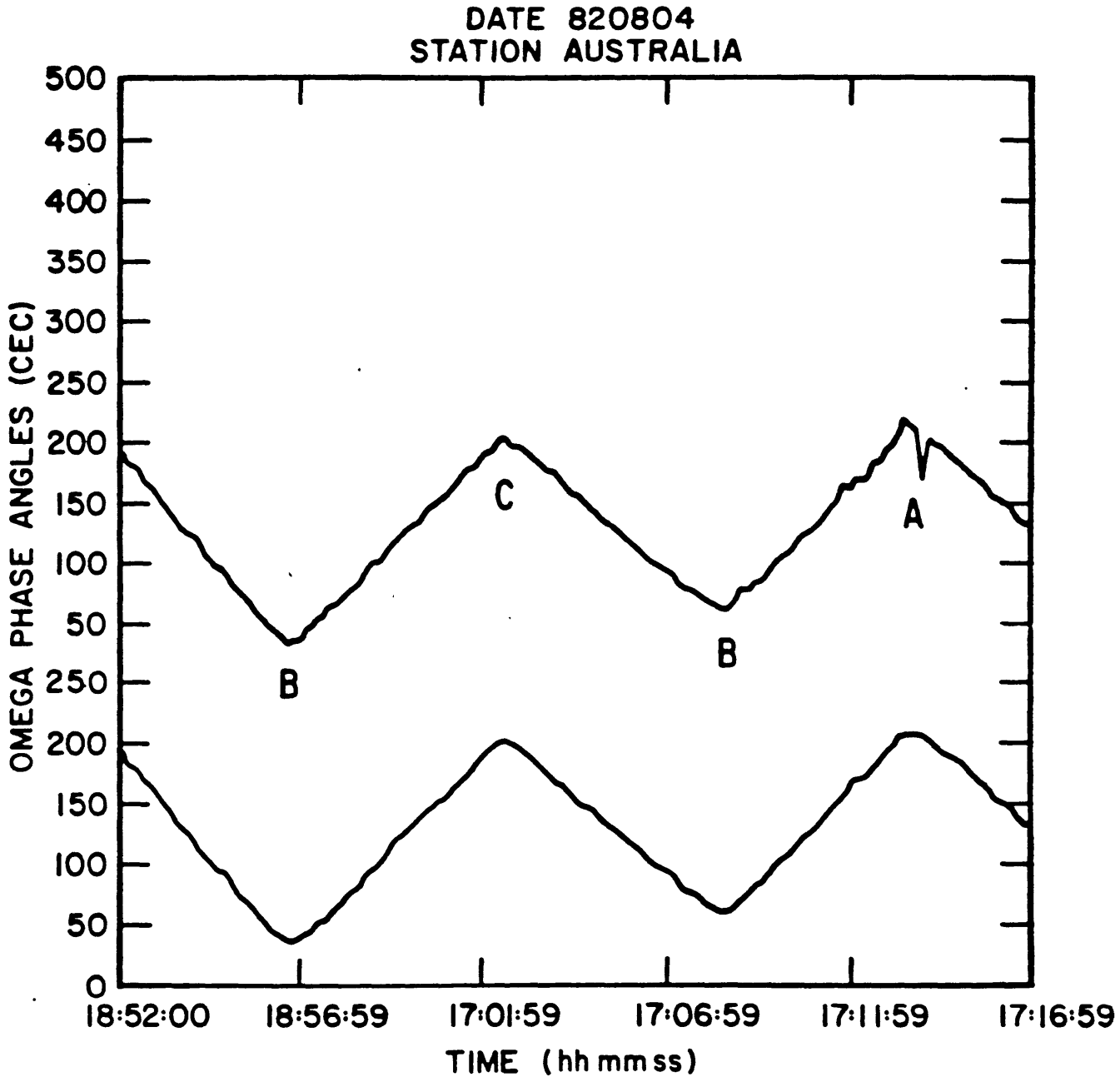

Figure 3. Same as figure 2, except for Australia.

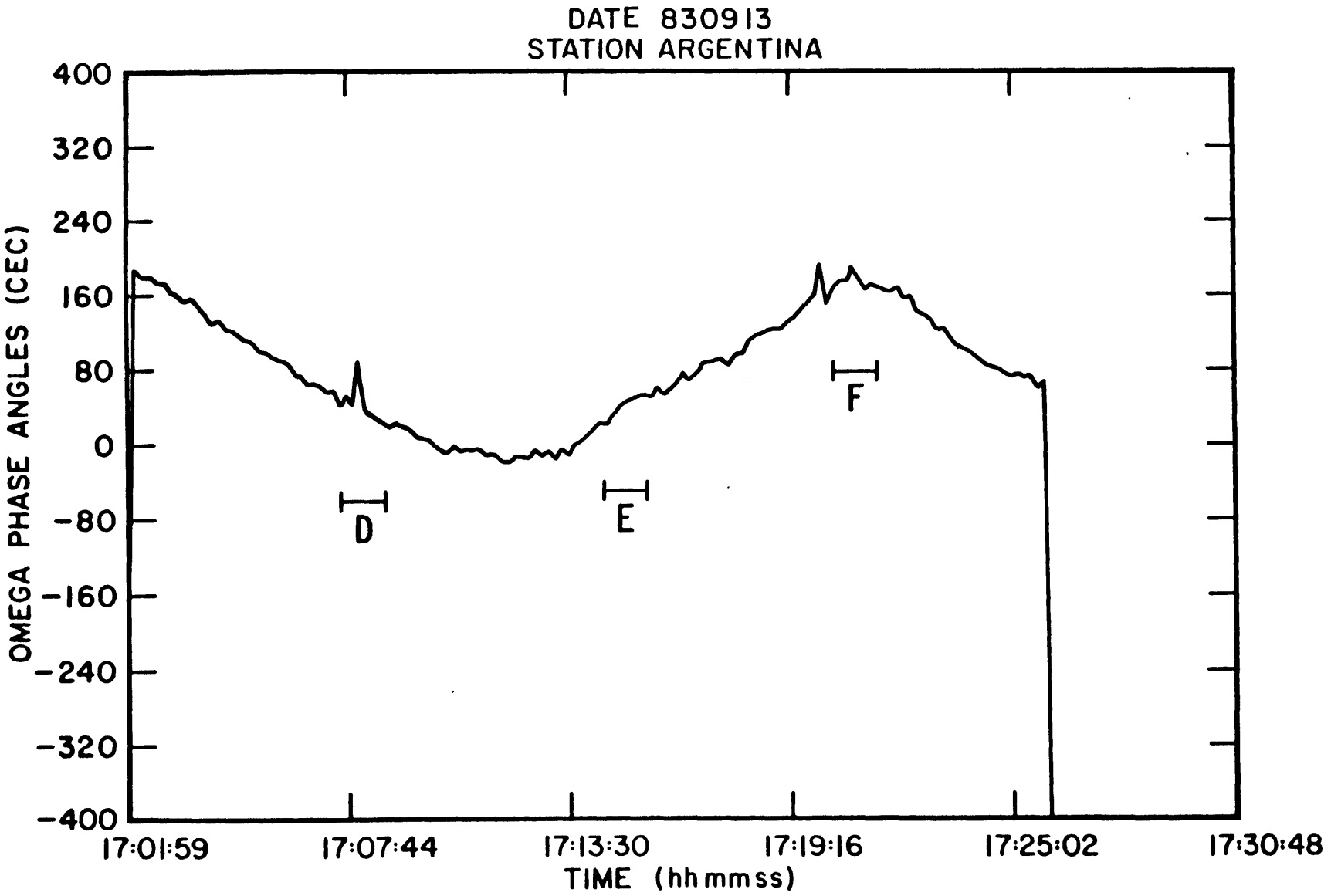

Figure 4. Raw Omega signals from the Argentina station during part of the 1983 mission. Turns are identified by the brackets and are labeled as in figure 1b.

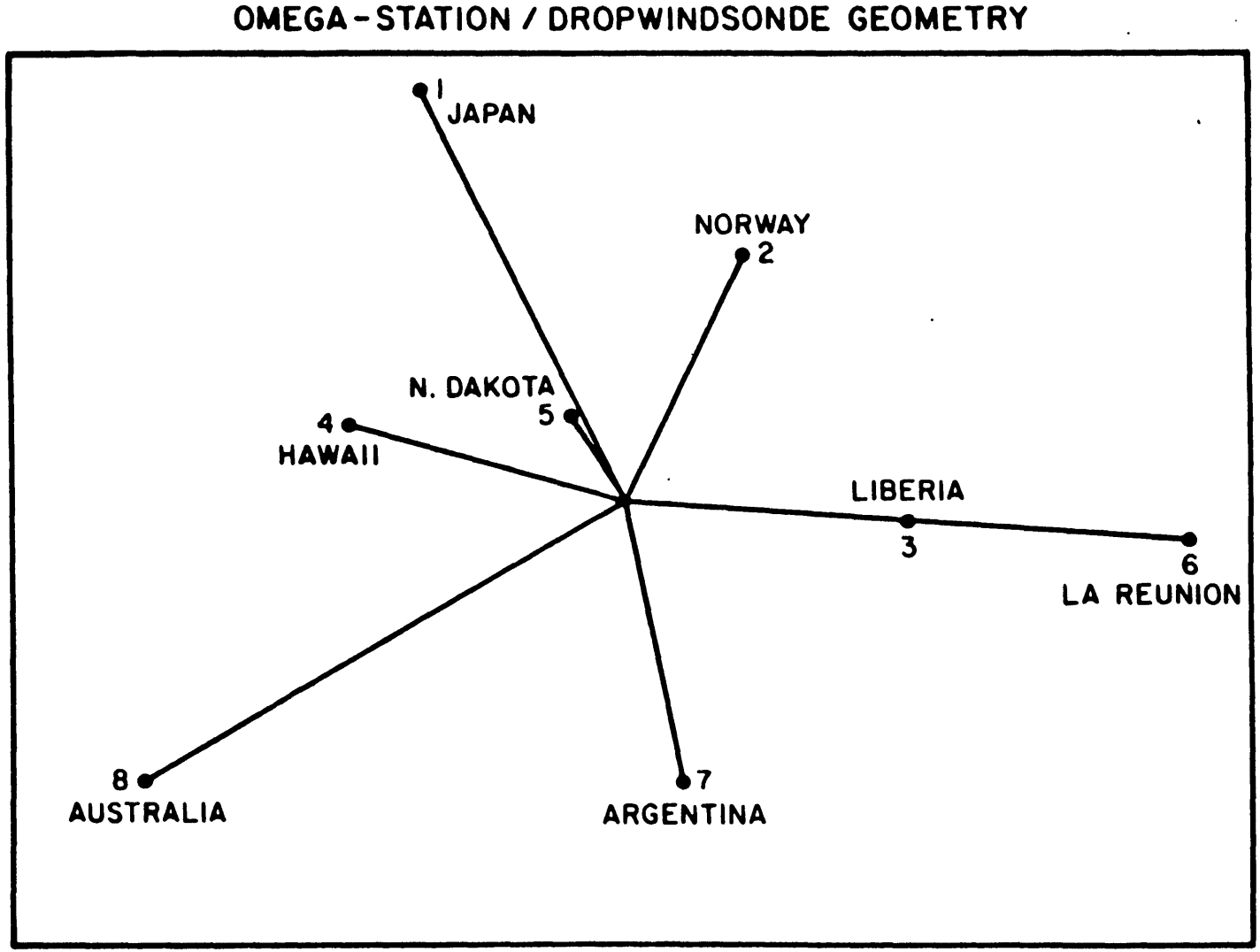

Figure 5. Relative station-sonde geometry for the research missions. The center of the diagram is near 25.7 N, 80.2 W.

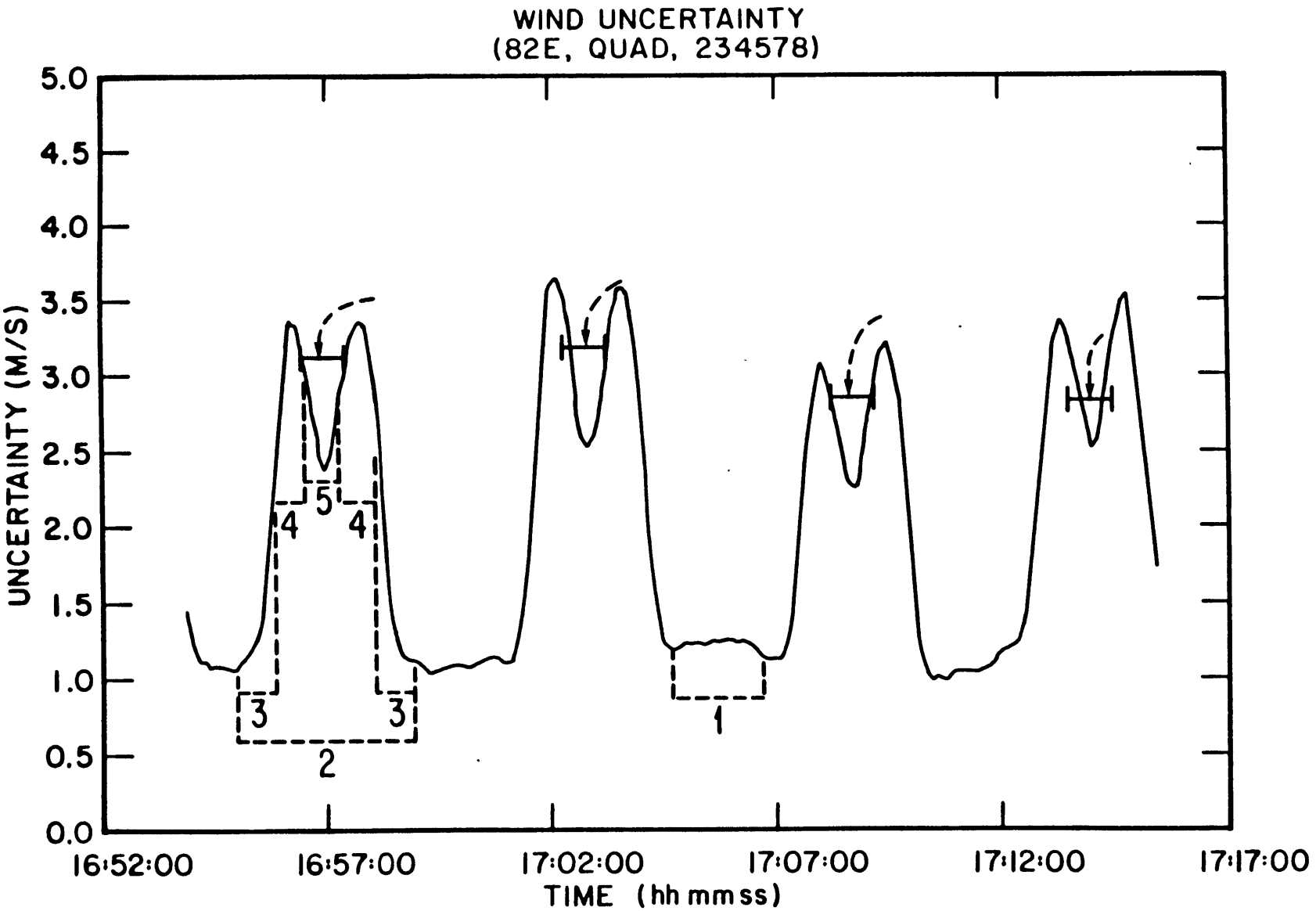

Figure 6. Wind uncertainty for a portion of wind profile (82E,QUAD,234578) (see text). Turns are identified by the arrows and brackets. Relative locations of the various classes of points are indicated by number: 1=leg, 2=turn, 3=turn edge, 4=turn peak, and 5=turn center.

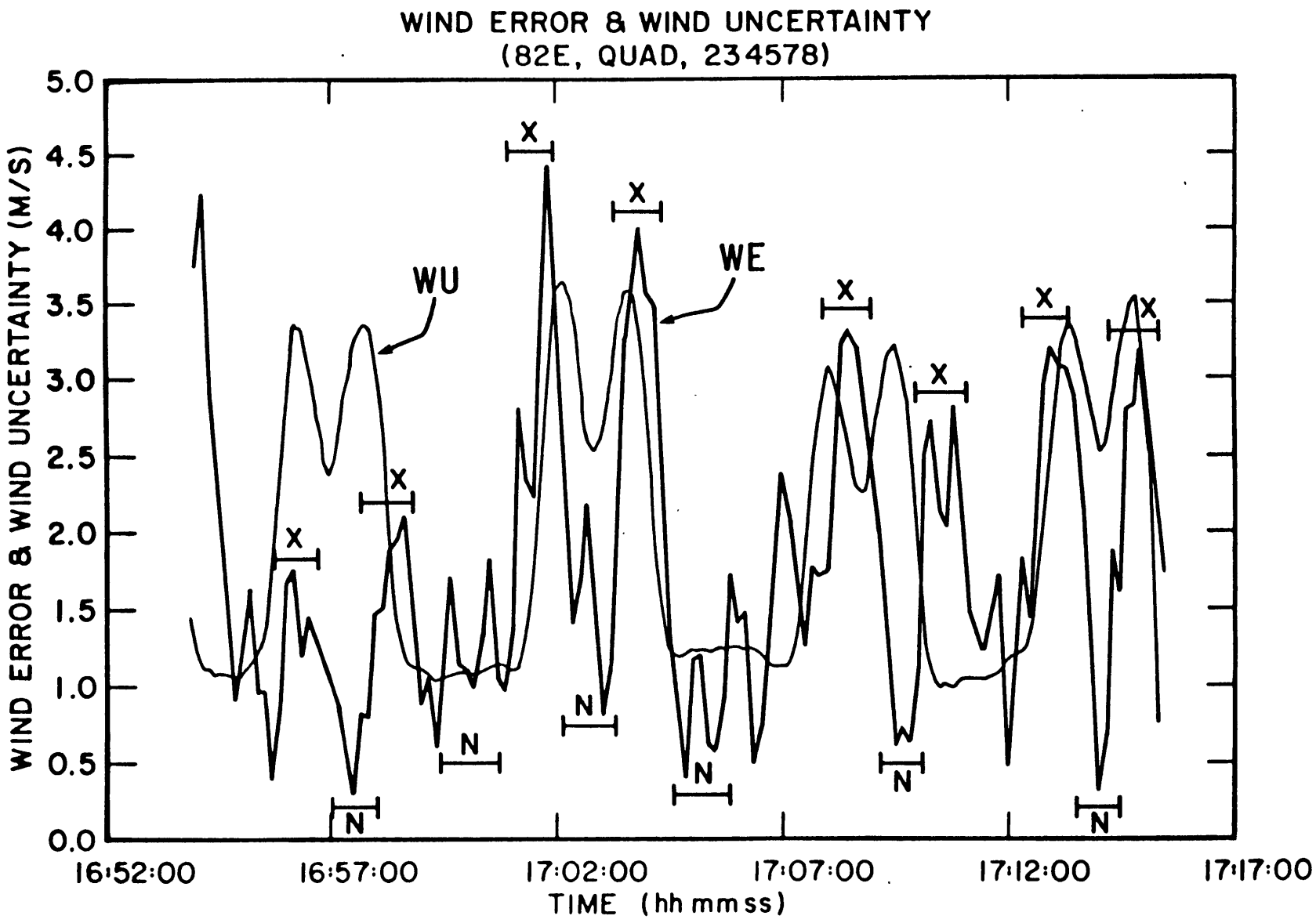

Figure 7. Wind uncertainty (thin line) and wind error (thick line) for the same profile as figure 6. Local maxima in wind error are identified by "x" and local minima by "n."

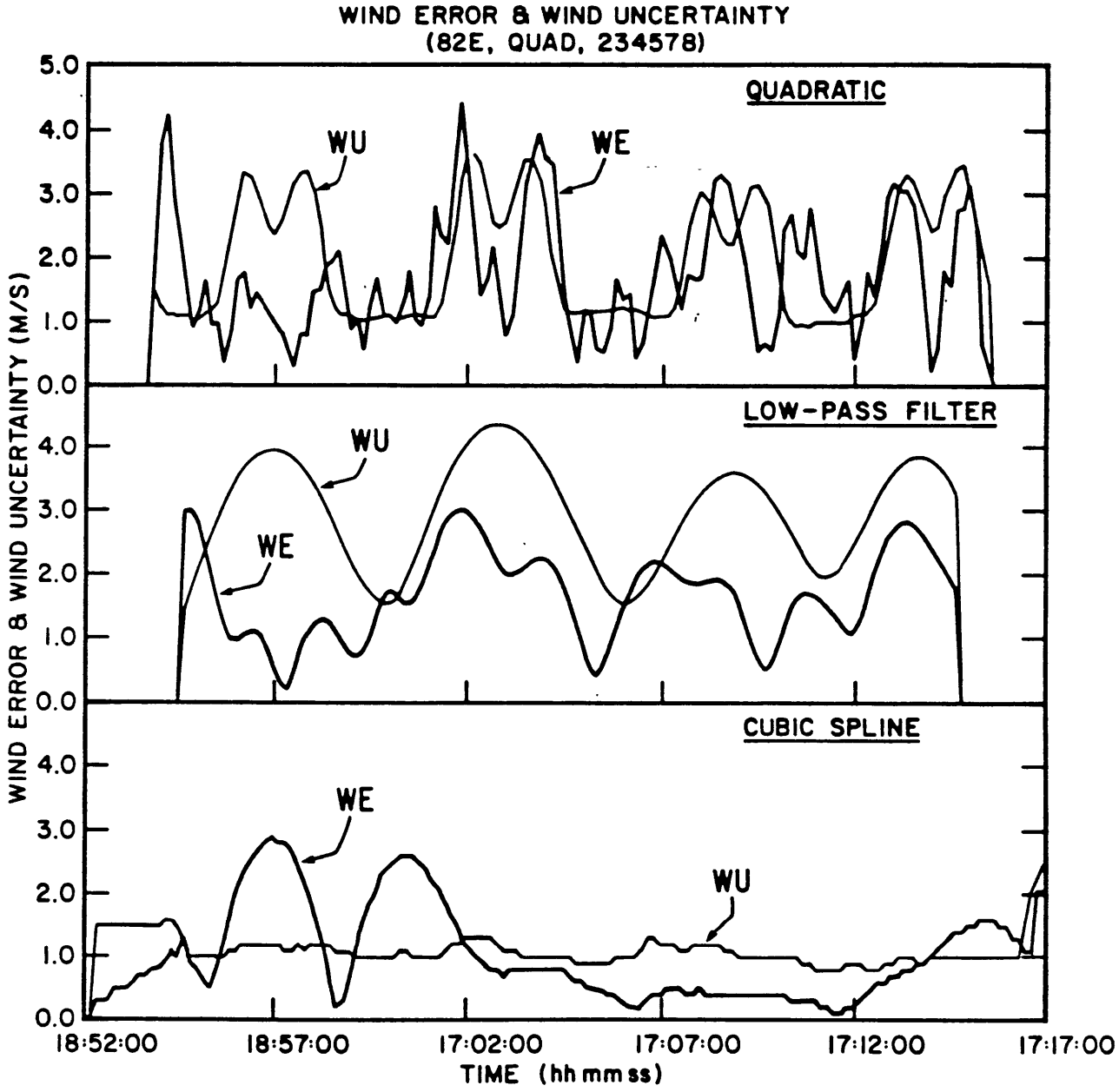

Figure 8. Wind uncertainty (thin line) and wind error (thick line) for a portion of the profiles (82E,234578) for the three windfinders.

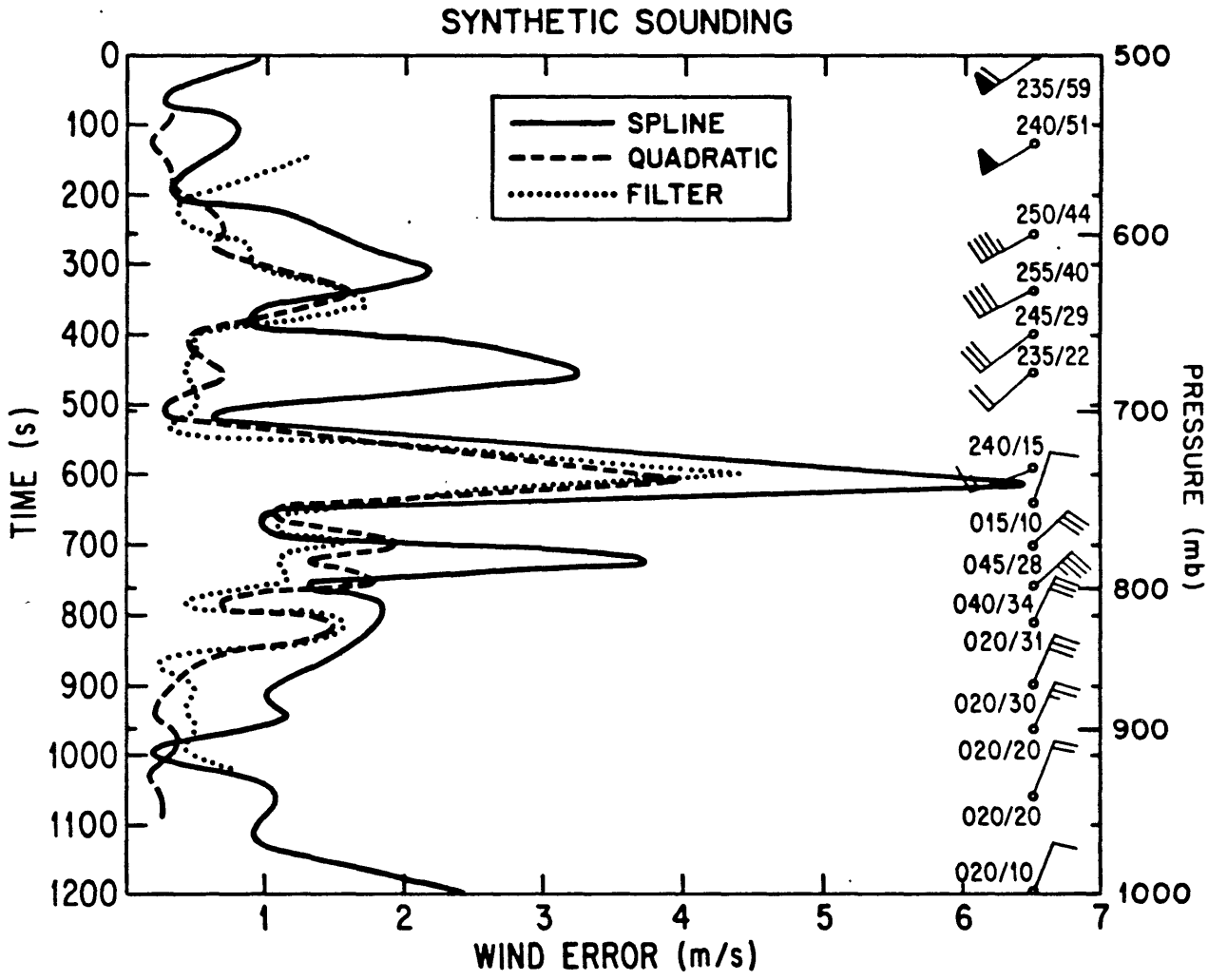

Figure 9. Wind profile of the synthetic sounding with associated wind errors for the three wind-finders. Rawinsonde data, from which synthetic Omega signals were derived, appear along the right side of the figure. Values of wind direction and speed (in knots) appear next to each plotted wind vector. Errors for each wind-finder in reproducing this sounding are given on the left side of the diagram.

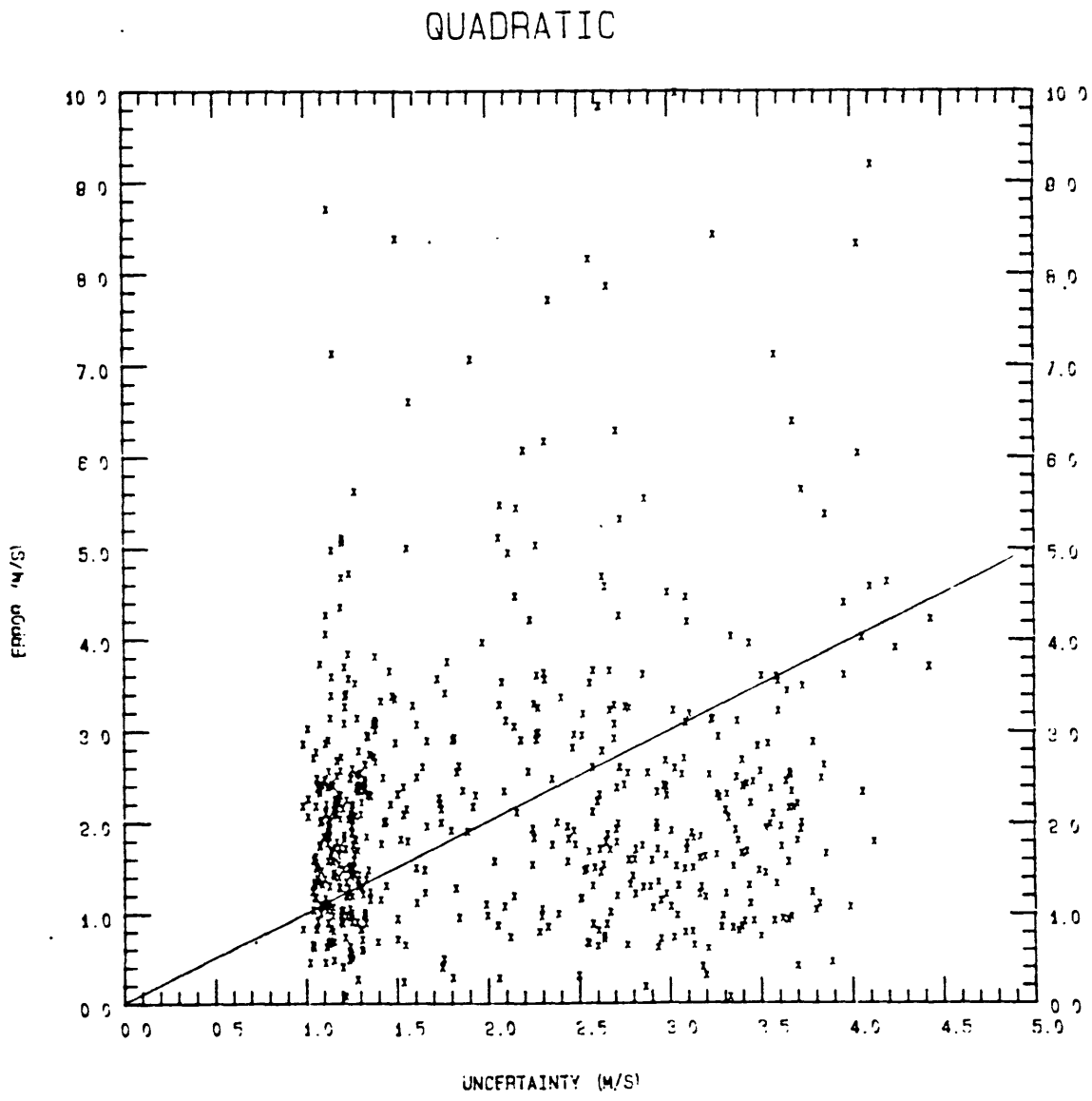

Figure 10. Scatter diagram for (82E,QUAD,234578). Each 10-s wind calculation is represented by an "x" in the diagram.

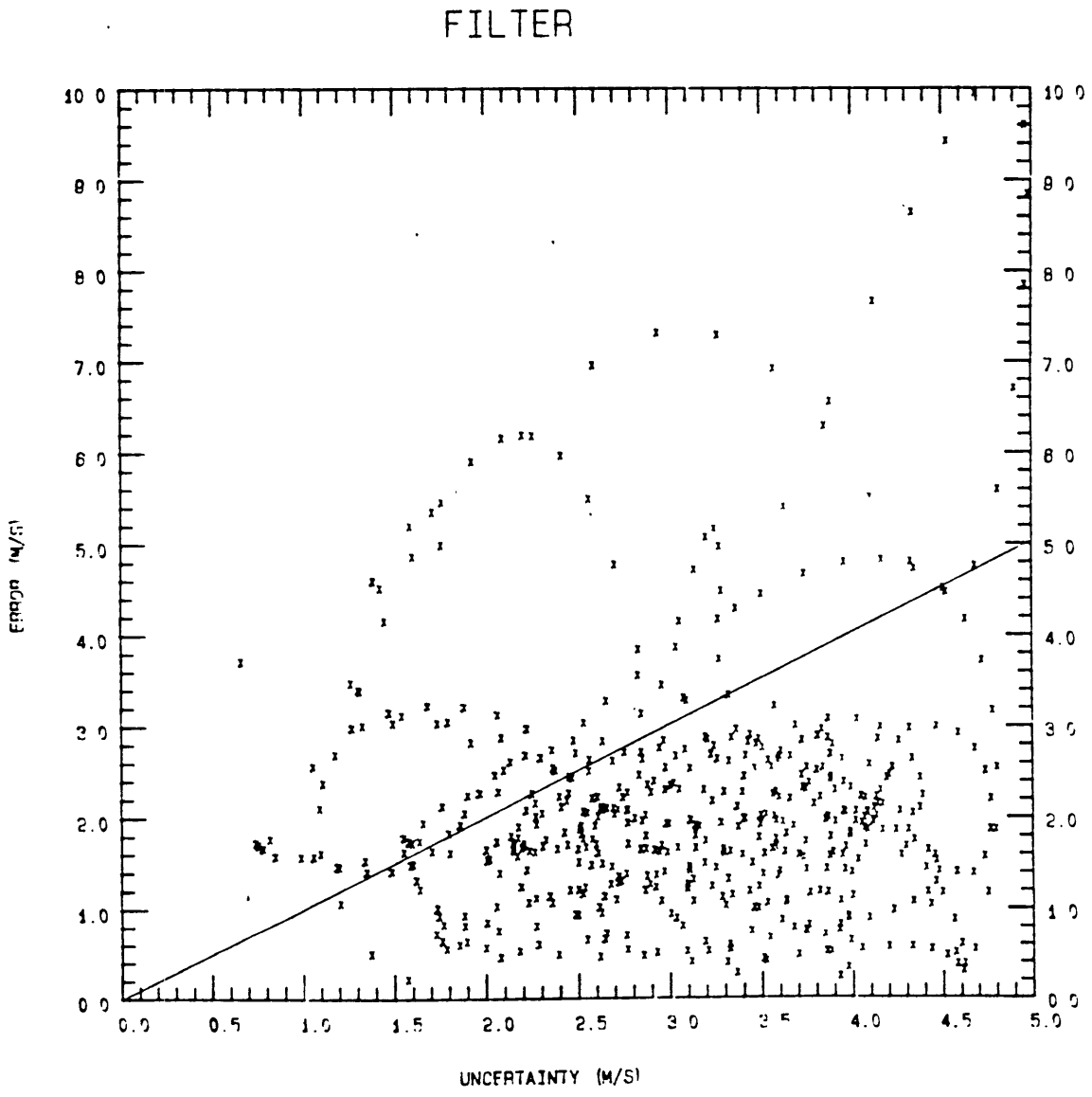

Figure 11. Same as figure 10, except for (82E,FIL,234578).

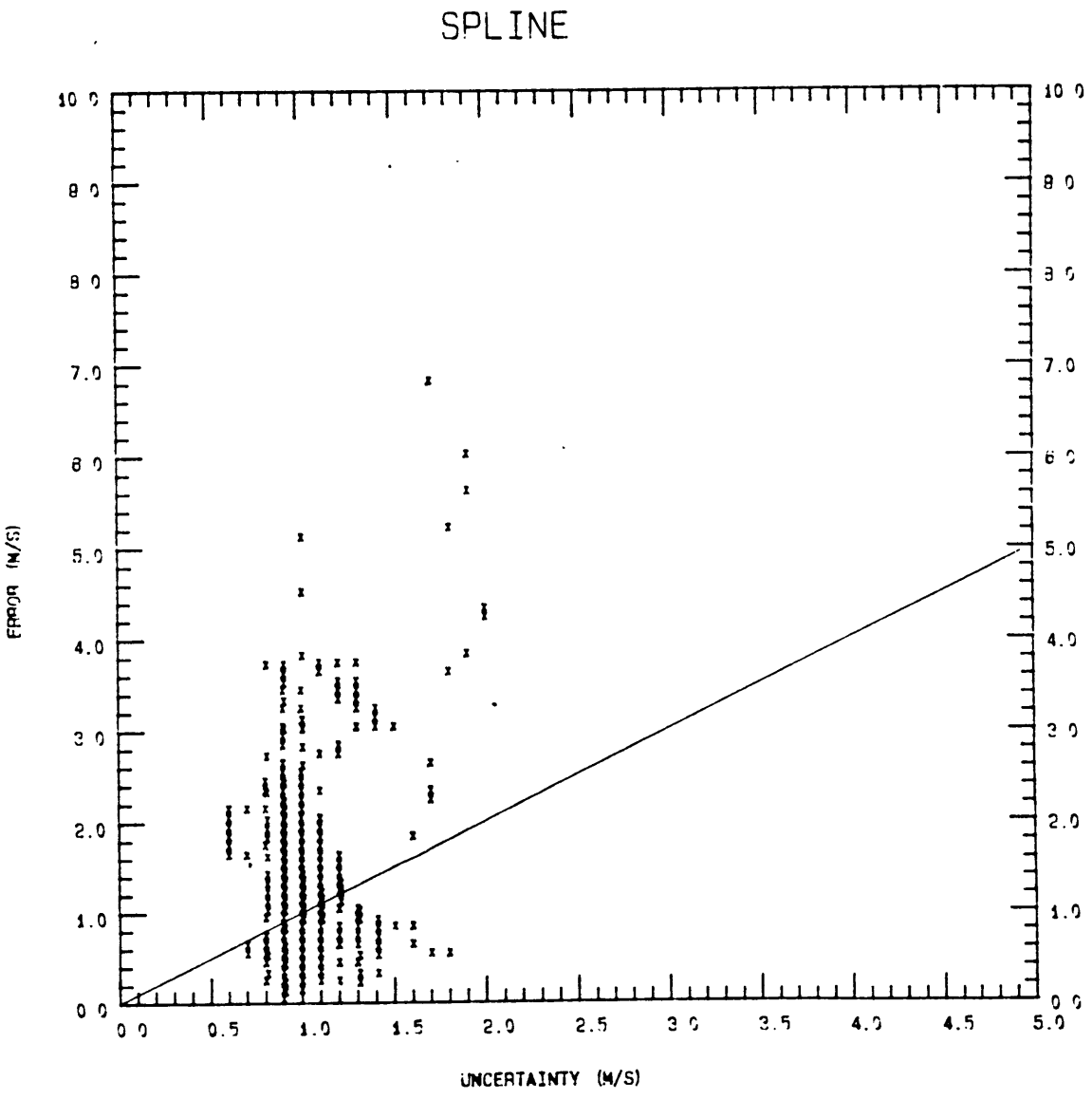

Figure 12. Same as figure 10 except for (82E,SPL,234578). Due to the precision of the uncertainty (0.1 m/s) the density of points in the lower left of the diagram does not appear as high as it should.

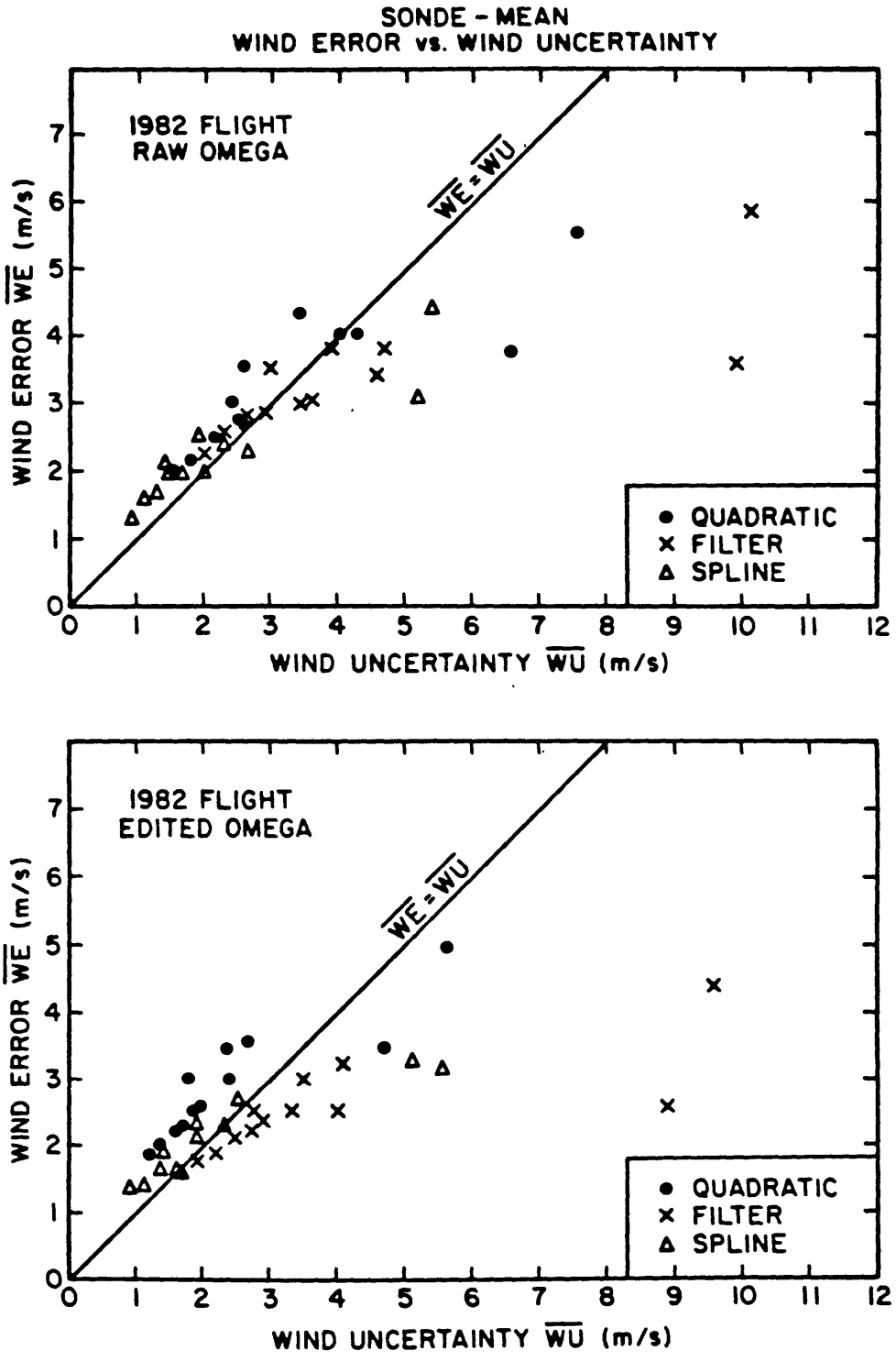

Figure 13. Sonde-mean values of uncertainty and error taken from table 4 (1982 flight) for raw Omega (top) and edited Omega (bottom).

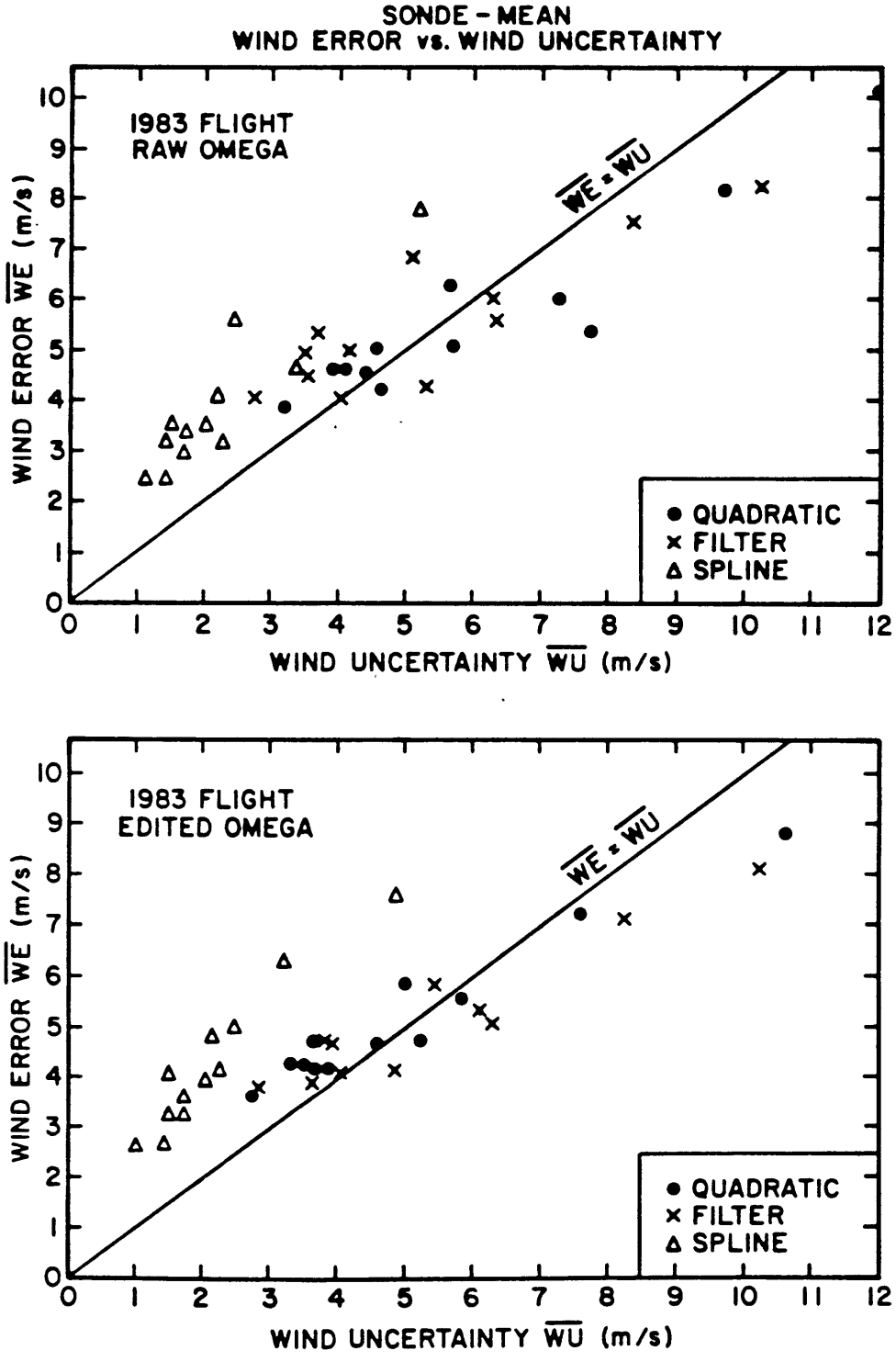

Figure 14. Same as figure 13, except for table 5 (1983 flight).

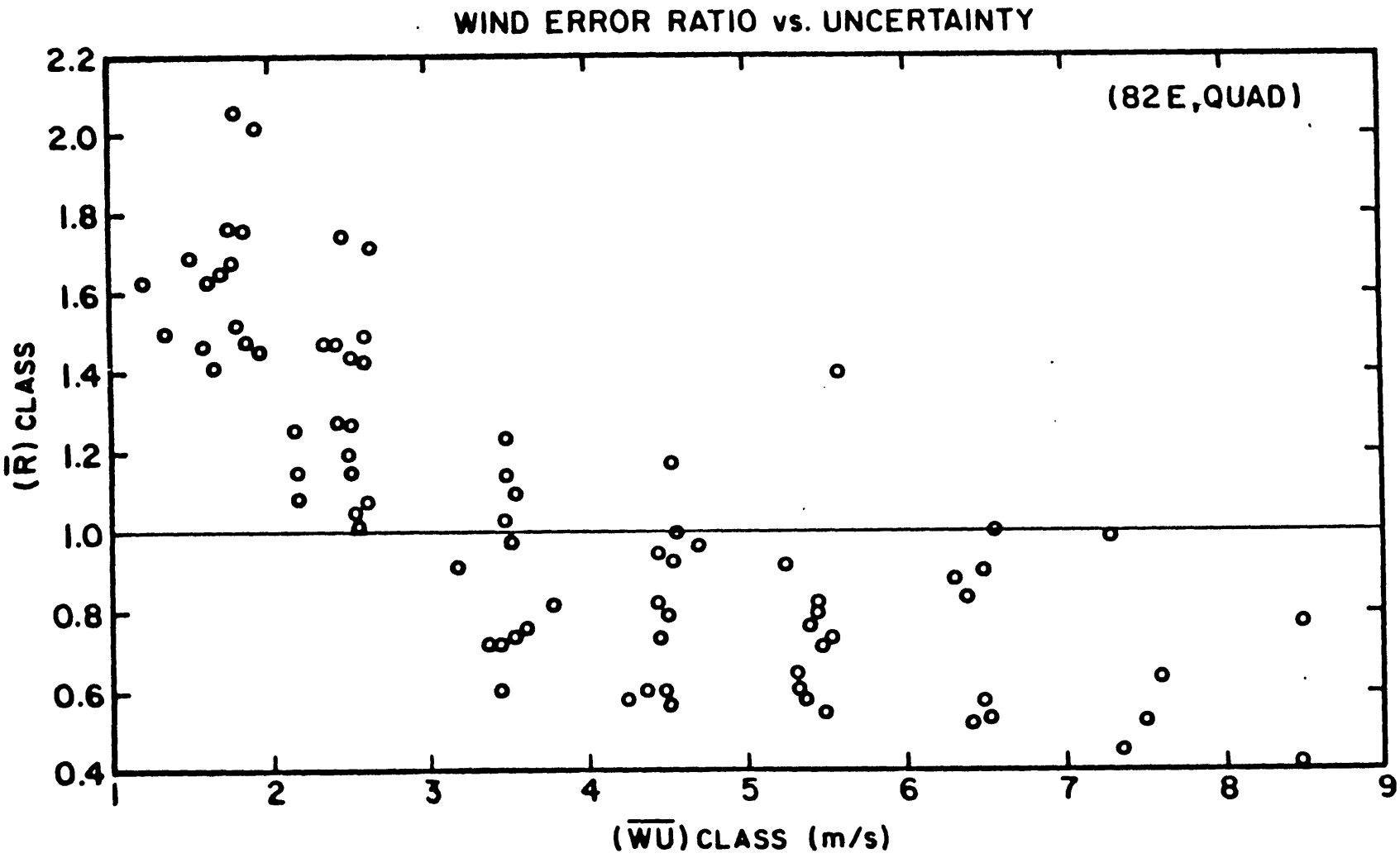

Figure 15. Class-mean values (see text) of uncertainty and error ratio for the 12 (82E,QUAD) profiles. All plotted points represent a minimum of 15 wind measurements.

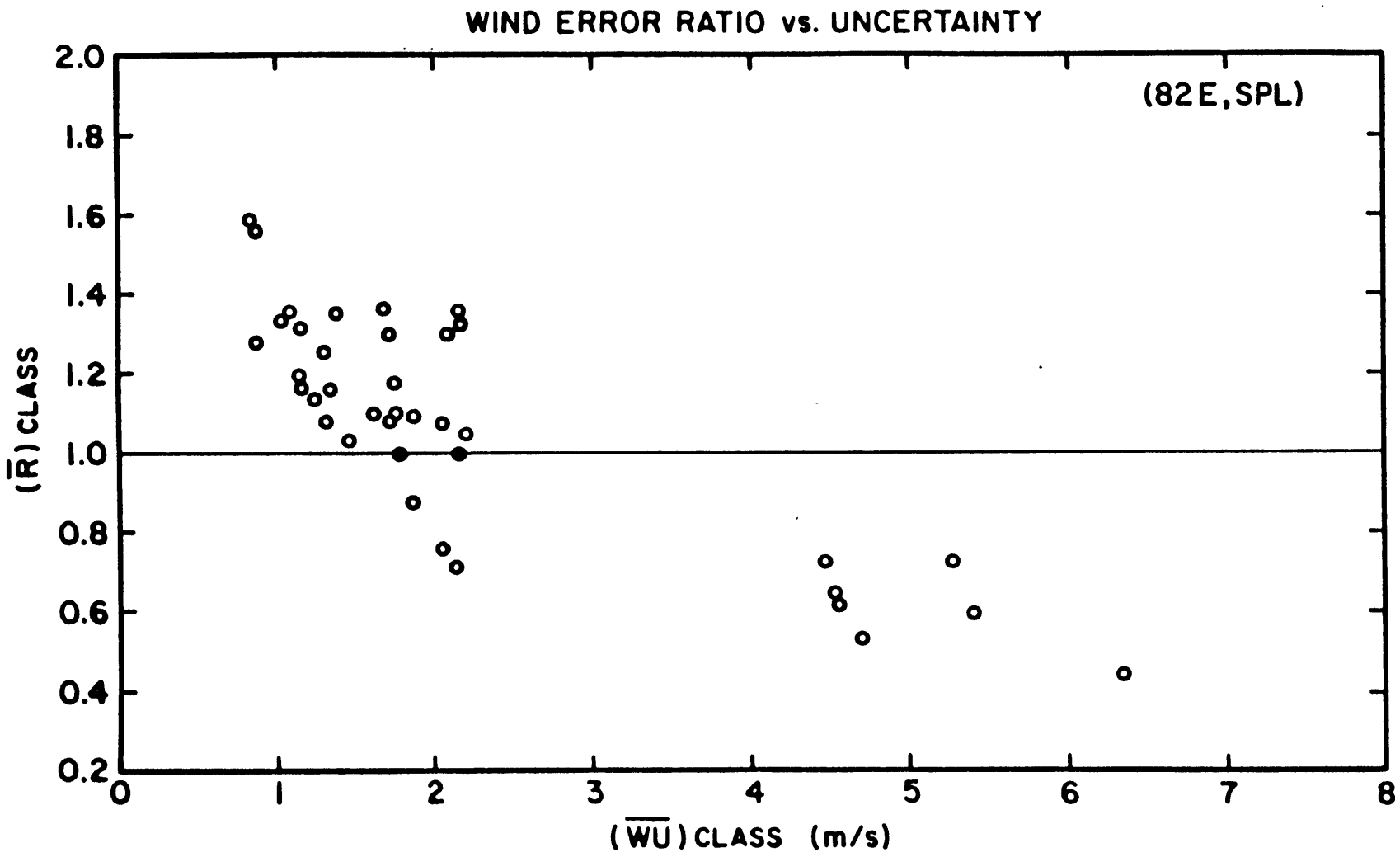

Figure 16. Same as figure 15, except for the (82E,SPL) profiles.

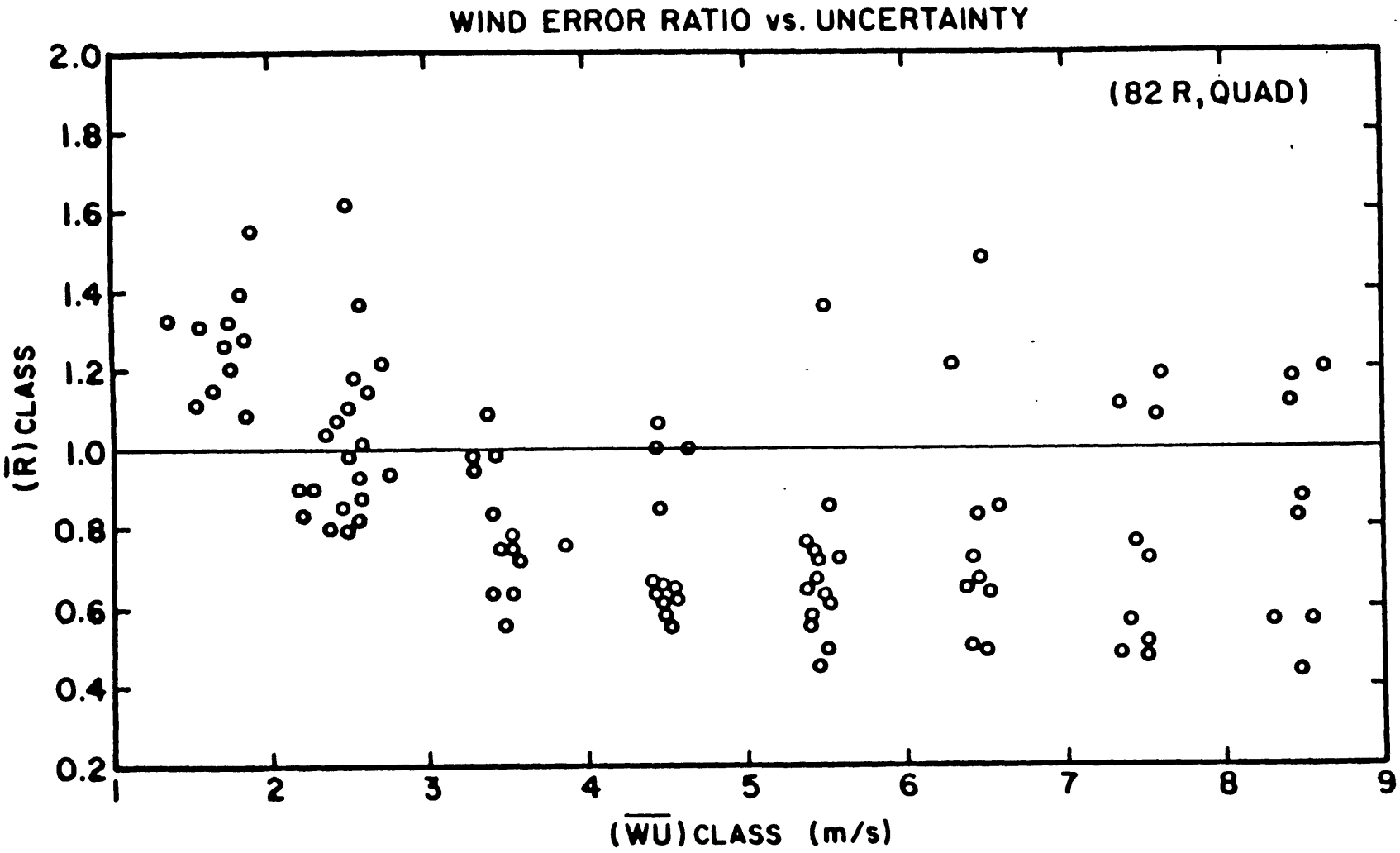

Figure 17. Same as figure 15, except for the (82R,QUAD) profiles.